Published March 26, 2012

Netrin instructs synaptic vesicle clustering through Rac GTPase, MIG-10, and the actin cytoskeleton

Andrea K.H. Stavoe and Daniel A. Colón-Ramos

Program in Cellular Neuroscience, Neurodegeneration and Repair, Department of Cell Biology, Yale University School of Medicine, New Haven, CT 06536

Netrin is a chemotrophic factor known to regulate a number of neurodevelopmental processes, including cell migration, axon guidance, and synaptogenesis. Although the role of Netrin in synaptogenesis is conserved throughout evolution, the mechanisms by which it instructs synapse assembly are not understood. Here we identify a mechanism by which the Netrin receptor UNC-40/DCC instructs synaptic vesicle clustering in vivo. UNC-40 localized to presynaptic regions in response to Netrin. We show that UNC-40 interacted with CED-5/DOCK180 and instructed CED-5 presynaptic localization. CED-5 in turn signaled through CED-10/Rac1 and MIG-10/Lamellipodin to organize the actin cytoskeleton in presynaptic regions. Localization of this signaling pathway to presynaptic regions was necessary for synaptic vesicle clustering during synapse assembly but not for the subcellular localization of active zone proteins. Thus, vesicle clustering and localization of active zone proteins are instructed by separate pathways downstream of Netrin. Our data indicate that signaling modules known to organize the actin cytoskeleton during guidance can be coopted to instruct synaptic vesicle clustering.

Introduction

Netrin is a chemotrophic factor originally discovered for its requirement in cell migration and axon guidance (Hedgecock et al., 1990; Ishii et al., 1992; Serafini et al., 1994). Genetic studies in *Drosophila* later indicated that the Netrin receptor Frazzled (homologous to *Caenorhabditis elegans* UNC-40 and vertebrate deleted in colorectal cancer [DCC]) is also required for short-range synaptic targeting (Winberg et al., 1998). Recent studies in *C. elegans* have also demonstrated that Netrin plays instructive roles in directing the formation of *en passant* presynaptic specializations (Colón-Ramos et al., 2007; Poon et al., 2008; Park et al., 2011). The capacity of Netrin to instruct synapse formation is also conserved in vertebrates (Manitt et al., 2009; Xu et al., 2010). How Netrin instructs these conserved roles in synapse formation and how these mechanisms relate to Netrin's canonical guidance role are not understood.

The capacity of guidance molecules to instruct synapse formation is not unique to Netrin. Many of the molecules originally identified for their roles in axon guidance, such as Ephrins, Semaphorins, and Slits, are now known to play important roles during synapse formation (Chen and Cheng, 2009; Shen and Cowan, 2010). Morphogenic signals such as Wnts can also spatially regulate the patterning of synaptic connections (Inaki et al., 2007; Klassen and Shen, 2007; Davis et al., 2008; Miech et al., 2008; Poon et al., 2008; Salinas and Zou, 2008). Although examples of guidance molecules controlling synapse formation abound, we understand less about how these molecules regulate synapse biology.

Here we use the *C. elegans* AIY interneuron to identify the molecular mechanisms that act downstream of the UNC-40 receptor to regulate synaptic vesicle clustering in vivo (Fig. 1 A). We show that core components of the canonical Netrin guidance pathway, such as Rac GTPases, have a novel role in synaptic vesicle clustering. We also demonstrate that CED-5 (a Rac guanine nucleotide exchange factor [GEF]) and MIG-10 (homologous to vertebrate proteins RIAM and Lamellipodin) localize to presynaptic regions in a Netrin-dependent manner. Our data indicate that Netrin instructs synaptic vesicle clustering

Correspondence to Daniel A. Colón-Ramos: daniel.colon-ramos@yale.edu

Abbreviations used in this paper: DCC, deleted in colorectal cancer; GEF, guanine nucleotide exchange factor.

Supplemental Material can be found at:
http://jcb.rupress.org/content/suppl/2012/03/21/jcb.201110127.DC1.html
http://jcb.rupress.org/content/suppl/2012/04/02/jcb.201110127.DC2.html

The Rockefeller University Press $30.00
J. Cell Biol. Vol. 197 No. 1 75–88
www.jcb.org/cgi/doi/10.1083/jcb.201110127

Published March 26, 2012

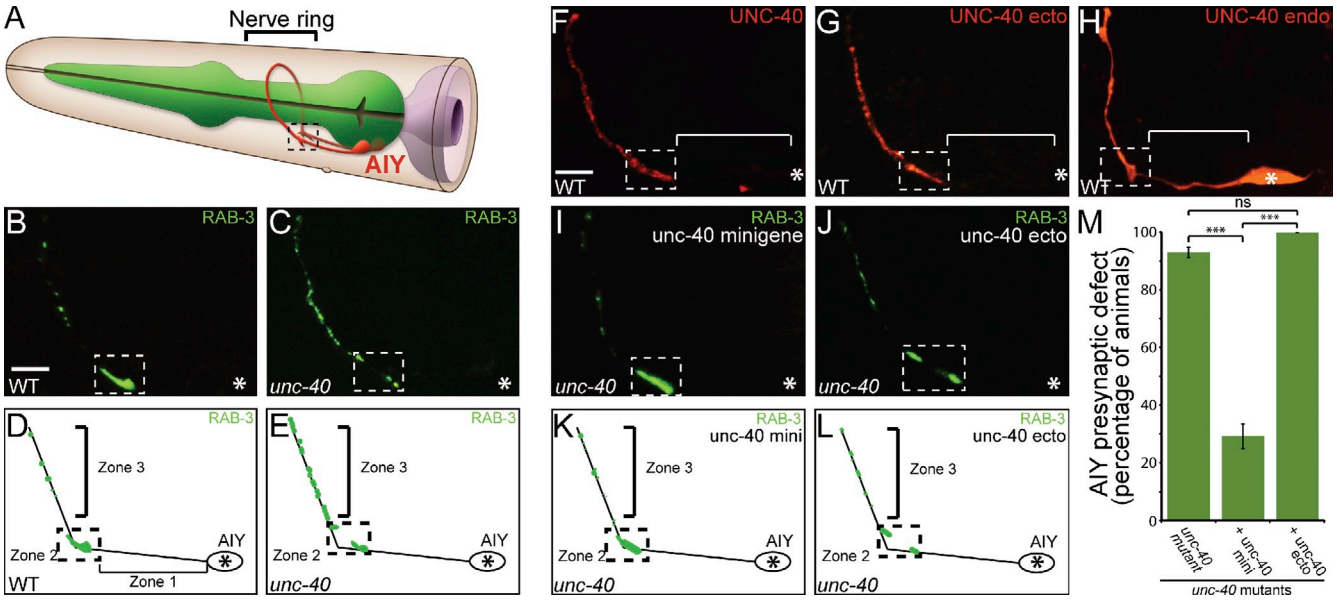

Figure 1. **The UNC-40 intracellular domain is required for instructing synaptic vesicle clustering in AIY.** (A) Schematic diagram of AIY morphology in the nerve ring (bracket). Dashed box represents Zone 2 of AIY where AIY:RIA synapses form (White et al., 1986). Modified image adapted from www.wormatlas.org with permission from Zeynep Altun. (B–E) Distribution of synaptic vesicles in AIY in wild-type (B and D) or *unc-40(e271)* (C and E) animals as visualized with GFP::RAB-3 and represented in cartoon diagrams (D and E). RAB-3::GFP marker used here has been shown to associate with vesicles during the late stage of the secretory pathway (Matteoli et al., 1991). Bar (B and C), 5 µm. (F and G) Localization of UNC-40::GFP (F) and UNC-40 ecto::mCh (G) expressed cell-specifically in AIY using the *ttx-3* promoter. Note the enrichment of UNC-40::GFP (F) and UNC-40 ecto::mCh (G) in Zones 2 and 3, but absent from asynaptic Zone 1 (bracket). Bar (F–J), 5 µm. (H) Localization of UNC-40 intracellular domain::mCherry expressed cell-specifically in AIY. Note diffuse localization throughout neurite, including Zone 1 (bracket, compare with F and G). Although expression of the endodomain in other neurons has been shown to cause gain-of-function outgrowth and guidance phenotypes (Gitai et al., 2003), we did not observe gain-of-function phenotypes in AIY resulting from expression of this construct (see Fig. S3, H and I). (I–L) *unc-40(e271)* mutant animals expressing an *unc-40* minigene (I and K) or an *unc-40* minigene lacking the intracellular domain (called unc-40 ecto; J and L). Presynaptic pattern was assayed with the GFP::RAB-3 probe in AIY. (M) Quantification of the AIY presynaptic phenotype in *unc-40(e271)* animals with the *unc-40* minigene or the *unc-40* ecto minigene. Error bars represent 95% confidence interval. In all images, asterisk represents location of the cell body and dashed box encloses AIY Zone 2; ***, $P < 0.0001$ between indicated groups by Fisher's exact test.

by directing the asymmetric localization of downstream signaling molecules that organize the actin cytoskeleton at synaptic sites.

Results

The intracellular domain of UNC-40 is required for synaptic vesicle clustering

The Netrin receptor UNC-40 has the conserved capacity to instruct synapse formation (Colón-Ramos et al., 2007; Poon et al., 2008; Manitt et al., 2009; Xu et al., 2010; Park et al., 2011). For example, in *C. elegans,* UNC-40 is cell-autonomously required for presynaptic assembly in the AIY interneurons (Fig. 1, B–E; Fig. S1, G–I; Fig. S2, G–I; Colón-Ramos et al., 2007). The role of UNC-40 in presynaptic assembly is not the result of a guidance role, as antero-dorsal guidance in AIY is not dependent on UNC-40 (Altun-Gultekin et al., 2001; Colón-Ramos et al., 2007). Furthermore, UNC-40 is localized to synaptic regions in response to Netrin (Fig. 1 F; Fig. S3 C; Colón-Ramos et al., 2007). These data suggest that local UNC-40 activity mediates presynaptic assembly.

To determine which domain of UNC-40 is required for synaptic vesicle clustering, we conducted structure-function studies. We generated "UNC-40 ectodomain::mCh", a transgene containing the intact transmembrane and ectodomains of UNC-40 with mCherry in lieu of the cytoplasmic domain (Fig. S3 A). We expressed this transgene cell-specifically in AIY and observed UNC-40 ectodomain::mCh enrichment in Zones 2 and 3, regions where presynaptic sites assemble (Fig. 1 G). The observed subcellular localization for the UNC-40 ectodomain is indistinguishable from that of full-length UNC-40 (Fig. 1 F). In addition, as observed for the full-length receptor, the localization of the ectodomain to Zones 2 and 3 is dependent on its ligand, UNC-6 (Fig. S3, C and G). These data suggest that the ectodomain is sufficient for UNC-40 localization to presynaptic sites in response to UNC-6.

To determine if the ectodomain is necessary for localization, we generated "UNC-40 endodomain::mCh" and expressed it cell-specifically in AIY. This transgene consists of the intact transmembrane and endodomains of UNC-40 fused to mCherry (Fig. S3 A). Consistent with the importance of the ectodomain in UNC-40 localization, we observed that the UNC-40 endodomain was not enriched in presynaptic regions. Instead, it displayed a diffuse localization pattern throughout the entire AIY neurite (Fig. 1 H). Overexpression of the endodomain in AIY did not alter AIY synaptic vesicle patterning (Fig. S3 H). Together, our data indicate that the UNC-40 ectodomain is both necessary and sufficient to instruct the localization of UNC-40 to presynaptic regions.

Given the capacity of the ectodomain to recapitulate the localization of the full-length receptor, we tested whether it was sufficient to rescue the synaptic vesicle clustering phenotype observed in *unc-40(e271)* mutants in AIY. To achieve this, we expressed the UNC-40 ectodomain under the endogenous *unc-40*

Published March 26, 2012

promoter in *unc-40(e271)* mutant animals. We then visualized the presynaptic specializations in Zone 2 and Zone 3 of AIY by cell-specifically expressing the presynaptic vesicle marker GFP::RAB-3. As previously reported, *unc-40(e271)* mutant animals display a highly penetrant presynaptic patterning defect in AIY (Fig. 1, C, E, and M; Colón-Ramos et al., 2007). Expression of full-length UNC-40 rescues the observed presynaptic patterning defect (Fig. 1, I, K, and M; Colón-Ramos et al., 2007). In contrast, we observed that expression of the UNC-40 ectodomain alone does not rescue the synaptic vesicle clustering defect in *unc-40(e271)* mutant animals (Fig. 1, J, L, and M). These data indicate that: (1) the ectodomain localizes to presynaptic sites in response to Netrin, but is not sufficient for rescue; and (2) the cytoplasmic domain of UNC-40 is required for instructing synaptic vesicle clustering in AIY, but is not sufficient for rescue.

The Rac-GEF CED-5 mediates synaptic vesicle clustering downstream of UNC-40

UNC-40 instructs synaptic vesicle clustering via its cytoplasmic domain, suggesting that molecules known to associate with this domain may be required for synaptic vesicle clustering. Genetic studies in *C. elegans* and biochemical studies in vertebrates show that Rac GTPases are activated in response to Netrin signaling via the UNC-40 cytoplasmic domain (Li et al., 2002a,b; Shekarabi and Kennedy, 2002; Gitai et al., 2003; Shekarabi et al., 2005; Quinn et al., 2008; Ziel et al., 2009). In vertebrates, Rac activation is mediated through the association of the UNC-40 homologue, DCC, with one of two GEFs, Trio (homologous to UNC-73) or DOCK180 (homologous to CED-5; Honigberg and Kenyon, 2000; Forsthoefel et al., 2005; Briançon-Marjollet et al., 2008; Li et al., 2008). We examined the genetic requirement of these two GEFs in AIY synaptic vesicle clustering. Mutation of *unc-73* resulted in severe axon outgrowth defects in AIY. We observed that 97.3% of the *unc-73(e936)* mutants failed to extend dorsally into the nerve ring (n = 148; Fig. S4, F and H). Our observations are consistent with other studies of the role of *unc-73* in AIY neurodevelopment (Altun-Gultekin et al., 2001). This phenotype for *unc-73(e936)* mutants is different from that observed for *unc-40(e271)* mutants, in which 93% of animals display correct axon guidance (Fig. S4 B; Altun-Gultekin et al., 2001; Colón-Ramos et al., 2007). The requirement of UNC-73 in axon outgrowth prevented us from assessing its role in synaptic vesicle clustering. Although we cannot discard a potential role for this GEF in synaptic vesicle clustering events, the observed outgrowth phenotype indicates that UNC-73 is involved in UNC-40–independent outgrowth events in AIY.

We next examined whether the DOCK180 homologue, CED-5, is required for correct AIY neurodevelopment. We examined three putative null alleles of *ced-5* (*n1812*, *tm1949*, *and tm1950)* and observed that unlike *unc-73(e936)* animals, *ced-5* mutants do not display axon guidance defects (Fig. S4, C, F, and I). We then examined synaptic vesicle markers in *ced-5* mutants. Like *unc-40(e271)* mutants, *ced-5* mutant animals displayed a highly penetrant presynaptic patterning defect as visualized using synaptic vesicle markers GFP::RAB-3 and SNB-1::YFP (Fig. 2, C and D; Fig. S1, J–L; Nonet, 1999). We found that 94.4% of *ced-5(n1812)* mutant animals have reduced synaptic vesicle clustering in Zone 2. Quantification of average fluorescence of GFP::RAB-3 revealed a twofold reduction as compared with wild-type animals in all synaptic regions (n = 108; Fig. 2, G and H; unpublished data). Interestingly, unlike *unc-40* mutants, *ced*-5 mutant animals do not display guidance or postsynaptic receptor distribution defects in postsynaptic partner RIA (Fig. S5, B and D–J). Thus, our data indicate that CED-5 is required for synaptic vesicle clustering in AIY. Our data also indicate that the UNC-40–mediated guidance mechanisms in RIA are genetically separable from the UNC-40–mediated synaptic vesicle clustering mechanisms in AIY.

ced-5 mutants phenocopy *unc-40* mutants, consistent with the hypothesis that these two molecules act in the same pathway to instruct synaptic vesicle clustering in AIY. To further test this hypothesis, we constructed a *ced-5(n1812);unc-40(e271)* double-mutant strain and visualized axon guidance and synaptic vesicle clustering in AIY. The *ced-5(n1812);unc-40(e271)* double mutant had enhanced guidance defects. For instance, 26.7% of the *ced-5(n1812);unc-40(e271)* double mutants exhibit AIY neurite truncations (n = 107). We analyzed the presynaptic pattern of *ced-5(n1812);unc-40(e271)* mutant animals that displayed normal guidance (Fig. 2 G). We observed that animals displaying normal guidance in the double mutants still displayed a presynaptic patterning defect that was similar to the presynaptic phenotypes seen in the single mutants; all displayed a reduction of synaptic vesicle clusters in the Zone 2 region and disorganized presynaptic sites in the Zone 3 region (Fig. 2, E and F). To further assay the phenotype, we quantified the average fluorescence in Zone 2 and observed that the reduction of synaptic vesicle clusters in the double-mutant animals is similar to that observed in *ced-5 (n1812)* single mutants (Fig. 2 H). We also observed that the reduction of average AIY total fluorescence in *unc-40(e271); ced-5(n1812)* mutants was similar to that of *ced-5* mutants (unpublished data).

The fact that the expressivity of the presynaptic patterning phenotype in the double mutant is qualitatively and quantitatively similar to that seen for the *ced-5* single mutants is consistent with our hypothesis that CED-5 acts downstream of UNC-40 to instruct synaptic vesicle clustering in AIY. To further examine the genetic interaction of CED-5 and UNC-40 in synaptic vesicle clustering, we built transheterozygotes of these alleles. *ced-5(n1812)* and *unc-40(e271)* are recessive alleles that, in heterozygote animals, predominantly display a wild-type phenotype in AIY. However, when we generated *ced-5/+;unc-40/+* transheterozygote animals, we observed that while AIY guidance was wild type, there was a significant enhancement of the percentage of animals displaying a synaptic vesicle clustering defect in AIY (Fig. 3 P). Together, our findings indicate that CED-5 and UNC-40 genetically interact to instruct synaptic vesicle clustering in AIY.

We had previously shown that local signaling by Netrin induces UNC-40 clustering at presynaptic regions and results in presynaptic assembly (Colón-Ramos et al., 2007). The source of Netrin in this region is a neuroglial cell (Wadsworth et al., 1996). Altering the position or morphology of these neuroglia affects UNC-40 localization and presynaptic assembly in AIY (Colón-Ramos et al., 2007). To understand how CED-5 interacts with UNC-40 in synaptic vesicle clustering, we first investigated

Published March 26, 2012

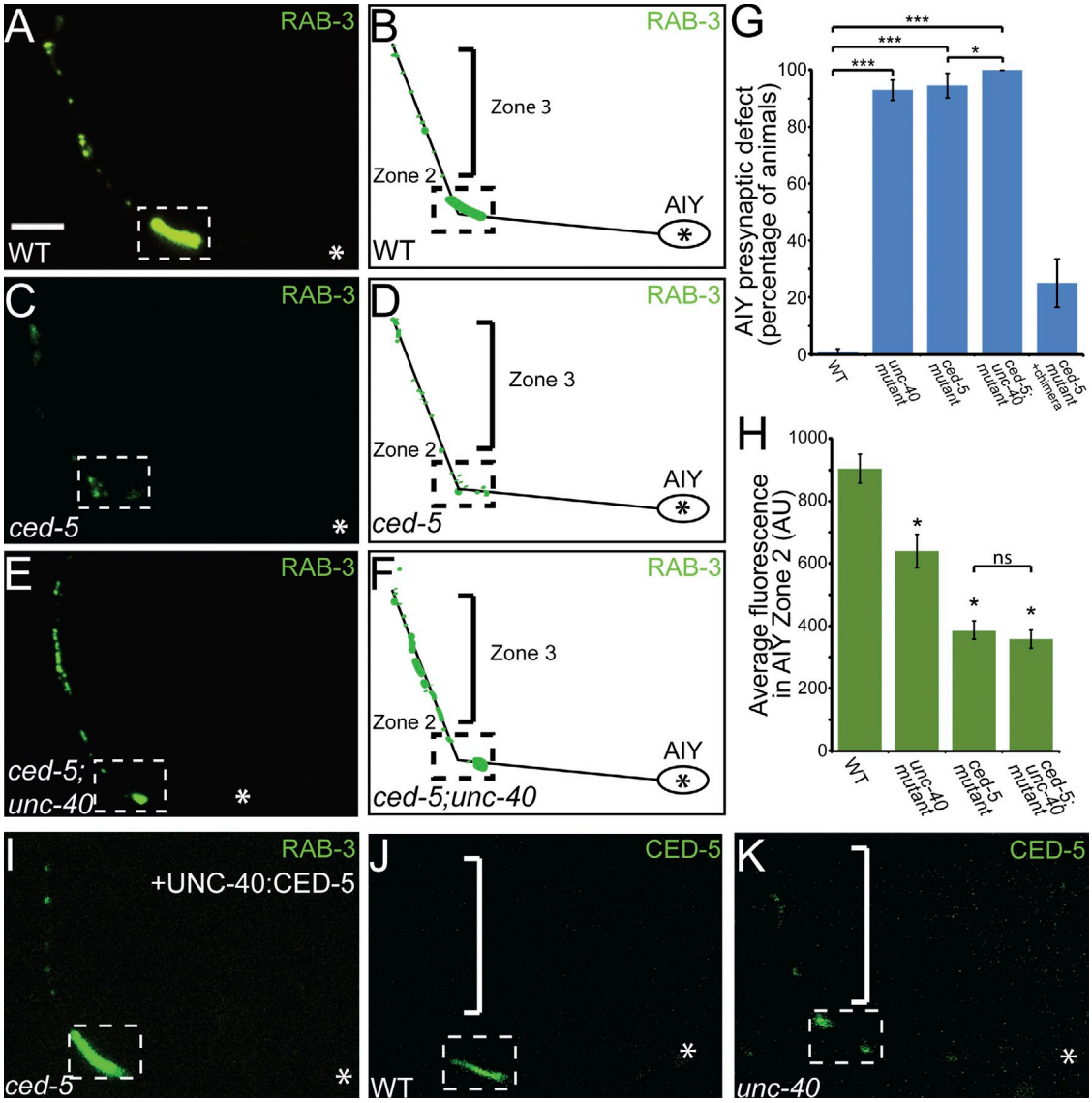

Figure 2. **The Rac GEF CED-5 is required downstream of UNC-40 for AIY synaptic vesicle clustering.** (A–F) Distribution of synaptic vesicles in AIY in wild type (A and B), *ced-5(n1812)* (C and D), and *ced-5(n1812);unc-40(e271)* (E and F) mutants. Note that the distribution of synaptic vesicles is disrupted in *ced-5(n1812)* and *ced-5(n1812);unc-40(e271)* double mutants compared with wild type. (G) Quantification of the percentage of animals displaying an AIY presynaptic defect in wild type (n = 318), *unc-40(e271)* (n = 299), *ced-5(n1812)* (n = 108), *ced-5(n1812);unc-40(e271)* (n = 105), and *ced-5(n1812)* + chimeric rescue construct UNC-40::CED-5 (n = 100). ***, $P < 0.001$ between indicated groups by Fisher's exact test. Error bars represent 95% confidence interval. (H) Quantification of the relative distribution of GFP::RAB-3 at the presynaptic Zone 2 (dashed box) in wild type (n = 25), *unc-40(e271)* (n = 37), *ced-5(n1812)* (n = 37), and *ced-5(n1812);unc-40(e271)* (n = 53) mutants (AU, arbitrary units). *, $P < 0.05$ between mutants and wild type by Fischer individual and Tukey simultaneous confidence intervals. Error bars represent SEM. (I) Distribution of synaptic vesicles in AIY in *ced-5(n1812)* mutants expressing the UNC-40:CED-5 chimera protein. Note that the synaptic vesicle clustering defect in *ced-5* mutants is significantly rescued with the chimera UNC-40::CED-5 construct (compare with C). (J and K) Confocal micrographs of animals expressing CED-5::GFP cell-specifically in AIY in wild-type (J) and *unc-40(e271)* mutant animals (K). Note that there is decreased CED-5::GFP signal in the *unc-40(e271)* mutants in Zone 2 (dashed box) relative to that in wild-type animals. In all images, asterisk represents location of the cell body and dashed box encloses AIY Zone 2. Bar, 5 µm.

whether the reported mutant backgrounds altered the morphology or position of the UNC-6–secreting neuroglia. When we visualized the UNC-6–secreting cell in the examined mutant backgrounds, we did not observe a change in the position or morphology of the neuroglia with respect to AIY, suggesting that the observed effects in synaptic vesicle clustering were not due to disruption of the morphology of the UNC-6–secreting cell (Fig. S4, A–E).

To understand the synaptic role of CED-5, we then examined its subcellular localization in AIY. To achieve this, we generated transgenes expressing CED-5::GFP cell-specifically in AIY. We observed that in wild-type animals, CED-5 is enriched in presynaptic Zone 2 (Fig. 2 J). We then examined if CED-5 enrichment in Zone 2 was dependent on UNC-40. Interestingly, we observed a decrease of CED-5::GFP localization to presynaptic regions in *unc-40(e271)* mutants, indicating that UNC-40 is required for CED-5 clustering in Zone 2 (Fig. 2 K). We did not detect any disruption in UNC-40::GFP localization in *ced-5(n1812)* mutants (Fig. S3 D). These cell biological data are consistent with our genetic analysis and further suggest that CED-5 acts downstream of UNC-40 in synaptic vesicle clustering.

Published March 26, 2012

In vertebrates, the CED-5 homologue, DOCK180, directly interacts with the endodomain of the UNC-40 homologue, DCC, to direct guidance (Li et al., 2008). Based on our genetic and cell biological data, we hypothesized that CED-5 directly interacts with the UNC-40 endodomain in AIY to instruct synaptic vesicle clustering. To test this hypothesis in vivo, we generated an UNC-40::CED-5 chimera, in which the CED-5 cDNA was fused in-frame with the full-length UNC-40 receptor at the C terminus. To determine if the direct interaction between UNC-40 and CED-5 was sufficient for instructing synaptic vesicle clustering, we examined the ability of this chimeric protein to rescue the *ced-5(n1812)* mutant phenotype in AIY. Indeed, we observed that expression of the chimeric transgene significantly rescued the AIY presynaptic patterning defect in *ced-5(n1812)* mutants (Fig. 2, G and I). Together, our data indicate that CED-5 localizes to presynaptic sites in response to UNC-40, where it instructs synaptic vesicle clustering.

CED-10 is required for synaptic vesicle clustering in AIY

In both vertebrates and invertebrates, the major targets of CED-5 are Rac GTPases (Kiyokawa et al., 1998; Nolan et al., 1998; Reddien and Horvitz, 2000; Lundquist et al., 2001). Therefore, we hypothesized that UNC-40 and CED-5 might regulate synaptic vesicle clustering through Rac GTPases. *C. elegans* has three Rac genes that interact with the CED-5 GEF during development to control neuronal cell migration and axon pathfinding: *ced-10*, *mig-2*, and *rac-2* (Fig. 3 A; Lundquist et al., 2001). In AIY, *mig-2(mu28)* and *rac-2(ok326)* mutant animals did not display cell migration or axon guidance defects (unpublished data). *ced-10(n3246)* mutants exhibited mildly penetrant outgrowth defects (16.2% of mutant animals had AIY truncations; $n = 148$), but in most animals, cell migration and axon guidance were wild type (Fig. S4, D, F, and J).

To examine the role of these Racs in AIY synaptic vesicle clustering, we visualized GFP::RAB-3 in loss-of-function mutants for each of these three Racs. *mig-2(mu28)* and *rac-2(ok326)* mutants did not display major defects in synaptic vesicle clustering (Fig. 3, D–G and N). However, *ced-10(n3246)* loss-of-function mutants displayed a highly penetrant presynaptic patterning defect as visualized using synaptic vesicle markers GFP::RAB-3, SNB-1::YFP, and SNG-1::YFP (98.4% of *ced-10(n3246)* animals, $n = 63$; Fig. 3, H, I, and N; Fig. S1, M–O; Fig. S2, J–L; Nonet, 1999; Zhao and Nonet, 2001). A weaker loss-of-function *ced-10* allele, *ced-10*(*n1993*), exhibited a similar phenotype (unpublished data). Our data suggest that MIG-2 and RAC-2 are not required for AIY development, but that CED-10 is required for synaptic vesicle clustering in AIY.

We then examined if CED-10 acts downstream of CED-5 and UNC-40 in synaptic vesicle clustering by assaying the presynaptic patterning defect in *ced-10(n1993);ced-5(n1812)* and *ced-10(n3246);unc-40(e271)* double mutants. Consistent with CED-10 acting in the same pathway as UNC-40 and CED-5, we observed that *ced-10(n1993);ced-5(n1812)* and *ced-10(n3246); unc-40(e271)* double mutants displayed phenotypes that were qualitatively similar to that seen for the *ced-10(n3246)* single mutants (Fig. 3, J–M).

To further examine the potential genetic interaction between UNC-40, CED-5, and CED-10 in synaptic vesicle clustering, we built transheterozygotes of these genes. *ced-10(n3246)* is a recessive allele and heterozygote animals predominantly display a wild-type phenotype. When we generated *ced-10/+;unc-40/+* and *ced-10/+;ced-5/+* transheterozygote animals, we observed a significant enhancement of the percentage of animals displaying synaptic vesicle clustering defects in AIY (Fig. 3 P). Together, our findings indicate that UNC-40, CED-5, and CED-10 interact to instruct synaptic vesicle clustering in AIY.

MIG-10 acts cell-autonomously in AIY to mediate synaptic vesicle clustering downstream of UNC-40

CED-10 acts through a number of effectors that regulate the actin cytoskeleton (Quinn and Wadsworth, 2008). One of them, UNC-115 (homologous to abLIM), interacts with Racs in axon pathfinding (Lundquist et al., 1998; Struckhoff and Lundquist, 2003). However, *unc-115(ky275)* mutants did not display major defects in synaptic vesicle clustering (Fig. 3 Q).

Another effector, MIG-10 (homologous to RIAM and Lamellipodin), is an evolutionarily conserved molecule that regulates actin polymerization and can directly bind to CED-10 (Fig. 4 A; Quinn et al., 2008). Interestingly, MIG-10 has been shown to asymmetrically localize in response to Netrin to mediate directional axon outgrowth and cell migration (Manser and Wood, 1990; Manser et al., 1997; Adler et al., 2006; Chang et al., 2006; Quinn et al., 2008).

We did not detect significant guidance or cell migration defects in *mig-10(ct41)* mutants in AIY (Fig. S4, E, F, and K). Instead, *mig-10(ct41)* mutants displayed a highly penetrant presynaptic patterning defect in AIY Zone 2 as visualized using synaptic vesicle markers GFP::RAB-3, SNB-1::YFP and SNG-1::YFP (87.9% of animals, $n = 141$; Fig. 4, C, E, and F; Fig. S1, P–R; Fig. S2, M–O). Additionally, quantification of the average GFP::RAB-3 fluorescence revealed that there was a statistically significant reduction of synaptic vesicle clusters when compared with wild-type animals (Fig. 4 G; unpublished data). Together, our data are consistent with a model in which UNC-40 instructs synaptic vesicle clustering in AIY through CED-5, CED-10, and MIG-10.

Because UNC-40 acts cell-autonomously in AIY to instruct presynaptic assembly (Colón-Ramos et al., 2007), we examined whether MIG-10 acts cell-autonomously in AIY to instruct synaptic vesicle clustering. To achieve this, we used a fosmid containing the *mig-10* gene. Expression of this rescuing fosmid in *mig-10(ct41)* mutant animals resulted in robust rescue of the AIY synaptic vesicle clustering defect (Fig. 4 H). To examine where MIG-10 functions to direct AIY synaptic vesicle clustering, we took advantage of the mitotic instability of the transgene arrays and analyzed *mig-10(ct41)* mosaic animals retaining the rescuing fosmid array in subsets of cells (Fig. 4 H; Yochem and Herman, 2003). We observed that mosaic animals retaining the array in AIY were rescued for the AIY presynaptic defect, whereas animals that did not retain the array in AIY, but retained it in other cells, such as postsynaptic partner RIA, did not show any detectable rescue of the AIY presynaptic defect (Fig. 4 H). Consistent with this result, we also observed that MIG-10 is expressed in AIY

Published March 26, 2012

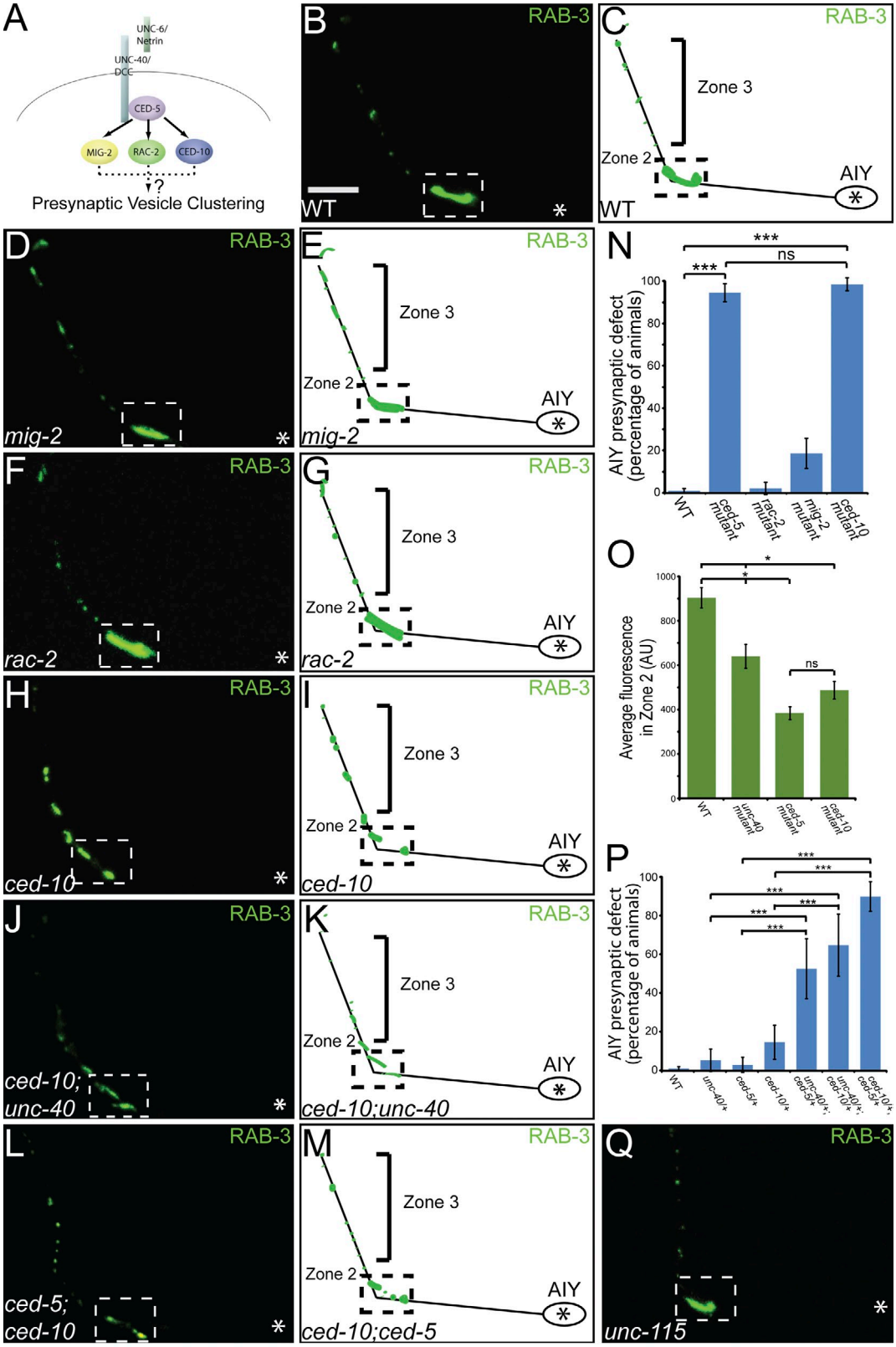

Figure 3. **The RacGTPase CED-10 is required for AIY synaptic vesicle clustering.** (A) Schematic of examined Rac GTPases downstream of CED-5. (B–M) Distribution of AIY synaptic vesicles in wild type (B and C), *mig-2(mu28)* (D and E), *rac-2(ok326)* (F and G), *ced-10(n3246)* (H and I), *ced-10(n3246);unc-40(e271)* (J and K), and *ced-10(n1993);ced-5(n1812)* (L and M) mutants. Note that distribution of synaptic vesicles is disrupted in *ced-10(n3246)*, *ced-10(n3246);unc-40(e271)*, and *ced-10(n1993);ced-5(n1812)* mutants compared with wild type. (N) Quantification of the percentage of animals displaying a disrupted AIY presynaptic pattern in wild type (n = 318), *ced-5(n1812)* (n = 109), *rac-2(ok326)* (n = 96), *mig-2(mu28)* (n = 113), and *ced-10(n3246)* (n = 63) mutants. ***, $P < 0.001$ between indicated groups by Fisher's exact test. Error bars represent 95% confidence interval. (O) Quantification of the relative distribution of GFP::RAB-3 at the presynaptic Zone 2 in wild type (n = 25), *unc-40* (n = 37), *ced-5* (n = 37), and *ced-10* (n = 39) mutants

Published March 26, 2012

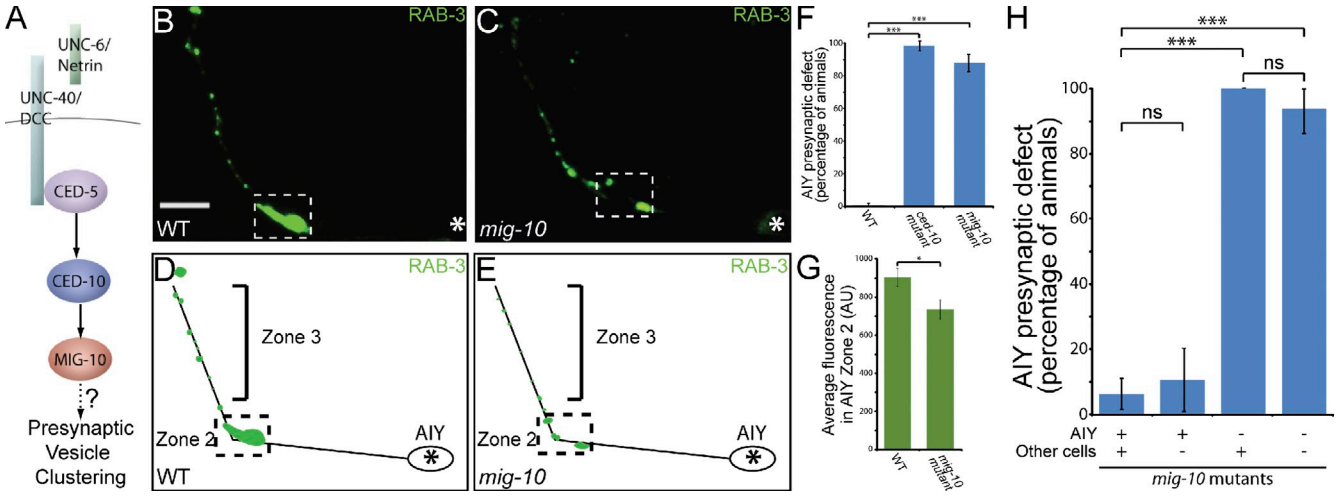

Figure 4. **MIG-10 is cell-autonomously required in AIY for synaptic vesicle clustering in Zone 2.** (A) Schematic of the pathway downstream of UNC-40. (B–E) Distribution of synaptic vesicles in AIY in wild type (B and D) and *mig-10(ct41)* (C and E) mutants. Note that the distribution of synaptic vesicles is disrupted in *mig-10(ct41)* mutants. Bar (B and C) 5 µm. (F) Quantification of the percentage of animals displaying a disrupted presynaptic pattern in AIY in wild type (n = 318), *ced-10(n3246)* (n = 63) and *mig-10(ct41)* (n = 141) mutants. ***, $P < 0.001$ between indicated groups by Fisher's exact test. Error bars represent 95% confidence interval. (G) Quantification of the relative distribution of GFP::RAB-3 at the presynaptic Zone 2 (dashed box) in wild type (n = 25) and *mig-10(ct41)* (n = 37) mutants (AU, arbitrary units). *, $P < 0.05$ between indicated groups by unpaired t test. Error bars represent SEM. (H) *mig-10(ct41)* mutant animals expressing an unstable transgene containing a *mig-10* rescuing fragment and cytoplasmic cell-specific markers in AIY and RIA were scored for retention of the transgene and rescue of the AIY presynaptic phenotype. Note that retention of the rescuing transgene in AIY, but not other cells (as determined by retention in RIA), results in rescue of the presynaptic defect. ***, $P < 0.001$ between indicated groups by Fisher's exact test. Error bars represent 95% confidence interval. In all images, asterisk represents the location of the cell body; dashed box encloses Zone 2.

(unpublished data). Additionally, similar to *ced-5* mutants, we did not observe guidance or postsynaptic patterning defects in the postsynaptic partner, RIA, in *mig-10(ct41)* mutants (Fig. S5, B, G, and L). Thus, our data indicate that *mig-10* acts cell-autonomously in AIY to instruct synaptic vesicle clustering.

To better understand how local signaling by Netrin results in synaptic vesicle clustering, we examined the subcellular localization of MIG-10 by generating a transgene expressing MIG-10 cDNA cell-specifically in AIY. We observed that MIG-10::GFP is enriched in presynaptic regions (Fig. 5 A). This localization is different from that seen for cytoplasmic expression of GFP (Fig. 5 B), but is reminiscent of CED-5::GFP localization (Fig. 2 J). Interestingly, MIG-10::GFP has previously been shown to localize asymmetrically during axon outgrowth in other neurons in response to Netrin (Adler et al., 2006; Quinn et al., 2008).

We next tested whether MIG-10 localization to presynaptic regions was dependent on UNC-6 and UNC-40 by visualizing MIG-10::GFP in *unc-6 (ev400)* and *unc-40(e271)* mutant backgrounds (Fig. 5, C and D). We observed a statistically significant decrease of MIG-10::GFP enrichment in presynaptic regions in *unc-6(ev400)* and *unc-40(e271)* mutants, suggesting that UNC-6 and UNC-40 are required for MIG-10 localization to presynaptic regions (Fig. 5 E). Conversely, there was no noticeable disruption in UNC-40::GFP localization in *mig-10(ct41)* mutants (Fig. S3 F). We also observed a statistically significant decrease of MIG-10::GFP enrichment in presynaptic regions in *ced-5(n1812)* and *ced-10(n3246)* mutant animals (Fig. 5 E). These cell biological data are consistent with our genetic analyses and reaffirm that MIG-10 acts downstream of UNC-6, UNC-40, CED-5, and CED-10 in synaptic vesicle clustering.

CED-5 and MIG-10 are not required for the localization of active zone proteins SYD-1 and SYD-2

UNC-40 is required for presynaptic assembly in the AIY interneurons, and *unc-40* mutant animals display a significant reduction of both synaptic vesicle clusters and active zone proteins at presynaptic sites (Fig. S1, G–I; Fig. S2, G–1; Fig. 6, A–D; Colón-Ramos et al., 2007). To determine if the examined downstream pathway was also required for the localization of active zone proteins to presynaptic sites, we visualized the subcellular localization of SYD-1::GFP and SYD-2::GFP (Fig. 6, A–H). SYD-1 and SYD-2 are evolutionarily conserved proteins that localize to active zones and are required for active zone assembly in a number of neurons, including AIY (Fig. 6, A, B, and J; unpublished data; Zhen and Jin, 1999; Hallam et al., 2002; Yeh et al., 2005;

(AU, arbitrary units). *, $P < 0.05$ between indicated groups by Fischer individual confidence intervals. Error bars represent SEM. (P) Transheterozygote analysis. Quantification of the percentage of animals displaying a disrupted presynaptic pattern in AIY in wild type (n = 318), *unc-40(e271)/+* heterozygotes (n = 57), *ced-5(n1812)/+* heterozygotes (n = 69), *ced-10(n3246)/+* heterozygotes (n = 62), *unc-40(e271)/+; ced-5(n1812)/+* transheterozygotes (n = 40), *unc-40(e271)/+;ced-10(n3246)/+* transheterozygotes (n = 34), and *ced-5(n1812)/+;ced-10(n3246)/+* transheterozygotes (n = 59). Note that a significant percentage of transheterozygote animals display synaptic vesicle clustering defects in AIY as compared with wild-type or heterozygote animals. ***, $P < 0.0001$ between indicated groups by Fisher's exact test. Error bars represent 95% confidence interval. (Q) Distribution of synaptic vesicles in *unc-115(ky275)* mutants. Note that the presynaptic pattern resembles that of wild-type animals (B). In all images, asterisk represents the location of the cell body; dashed box encloses Zone 2. Bar, 5 µm.

Published March 26, 2012

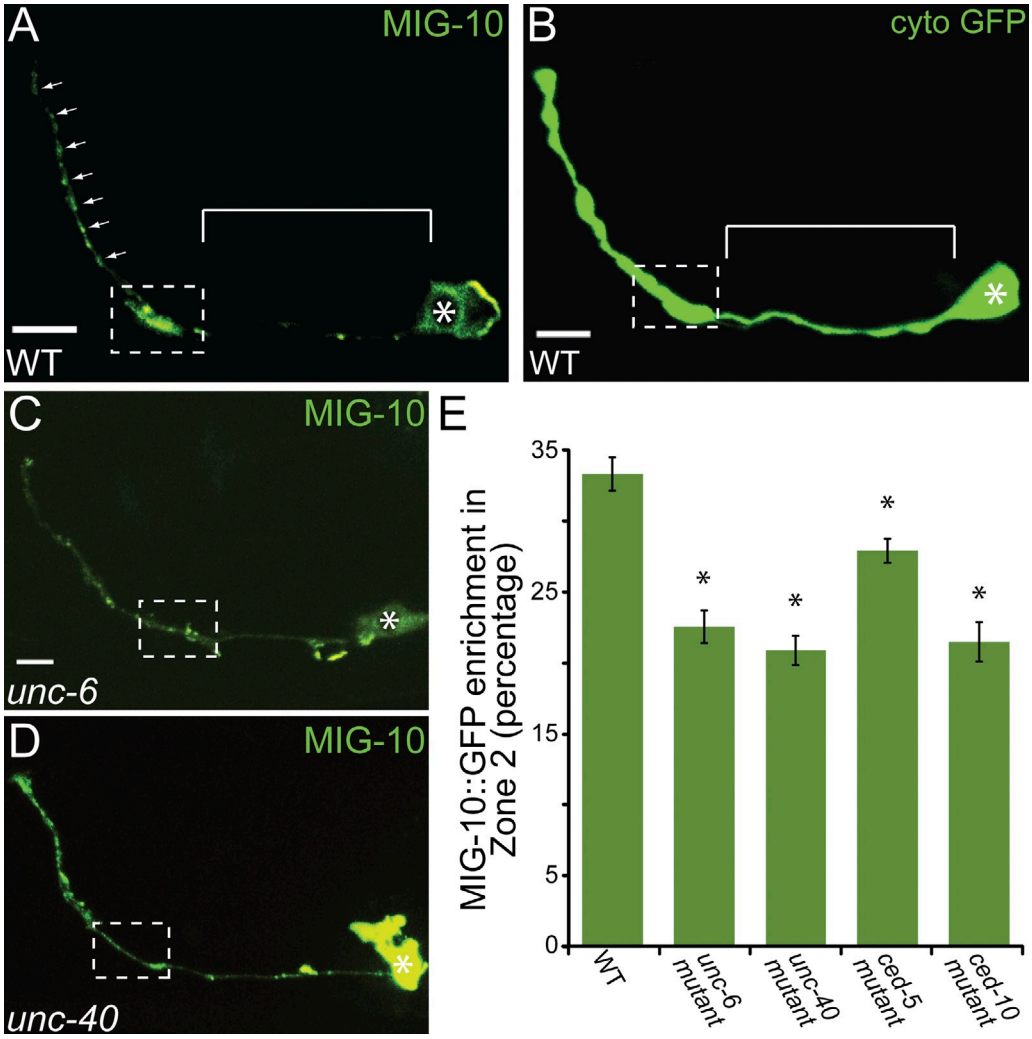

Figure 5. **MIG-10 localizes to presynaptic regions in response to Netrin.** (A) Confocal micrograph showing MIG-10::GFP subcellular localization cell-specifically in AIY. Bar, 5 µm. (B) Confocal micrograph showing cytoplasmic GFP expressed cell-specifically in AIY. Note that cytoplasmic signal is diffuse throughout the neurite, including Zone 1 (B, bracket), whereas MIG-10 is enriched in presynaptic regions (A, dashed box and arrows). Bar, 5 µm. (C and D) Confocal micrographs showing MIG-10::GFP subcellular localization expressed cell-specifically in AIY in *unc-6(ev400)* (C) and *unc-40(e271)* (D) mutant animals. Note that MIG-10::GFP is less enriched in Zone 2 in the two mutant backgrounds, as compared with wild-type animals (A). Bar (C and D), 5 µm. (E) Quantification of the relative MIG-10::GFP distribution in AIY presynaptic Zone 2 region in wild type ($n = 49$), *unc-6(ev400)* ($n = 31$), *unc-40(e271)* ($n = 18$), *ced-5(n1812)* ($n = 43$), and *ced-10(n3246)* ($n = 17$) mutant animals. *, $P < 0.05$ between mutants and wild type by Fischer Individual and Tukey simultaneous confidence intervals. Error bars represent SEM. Dashed box encloses AIY Zone 2 and asterisk represents location of the cell body.

Dai et al., 2006; Patel et al., 2006; Jin and Garner, 2008). Interestingly, although UNC-40 is required for the subcellular localization of SYD-1::GFP and SYD-2::GFP to presynaptic sites, we could not detect defects in the subcellular localization of these active zone proteins in *ced-5(n1812)* or *mig-10(ct41)* mutants (Fig. 6, A–H). In addition, we observed that although *syd-1(ju82)* and *mig-10(ct41)* single mutants both display highly penetrant synaptic vesicle clustering defects, the expressivity of the defects is qualitatively different. When we created a *syd-1(ju82); mig-10 (ct41)* double mutant, we observed an enhancement of the vesicle clustering defects as compared with the single mutants (Fig. 6, J–L). Together, our data indicate the existence of a parallel pathway downstream of UNC-40 required for localization of active zone proteins to presynaptic sites. Our data also suggest that the mechanisms that instruct active zone formation and synaptic vesicle clustering downstream of UNC-40 are genetically separable.

Netrin instructs F-actin accumulation at presynaptic sites

Our data indicate that Netrin instructs synaptic vesicle clustering through a Rac GTPase and MIG-10. These molecules have the shared capacity to induce local changes in cytoskeletal dynamics by regulating actin polymerization (de Curtis, 2008; Quinn and Wadsworth, 2008; Quinn et al., 2008). A number of studies have shown that disruption of F-actin specifically during synaptogenesis results in fewer presynaptic assemblies, indicating a role for F-actin during synaptogenesis (Colicos et al., 2001; Zhang and Benson, 2001, 2002; Sankaranarayanan et al., 2003; Lucido et al., 2009). Therefore, we hypothesized that CED-5, CED-10, and MIG-10 are required downstream of Netrin to organize the actin cytoskeleton in presynaptic regions (Fig. 7 A).

To examine this hypothesis, we visualized F-actin in AIY by cell-specifically expressing the in vivo F-actin probe UtrCH::GFP

Published March 26, 2012

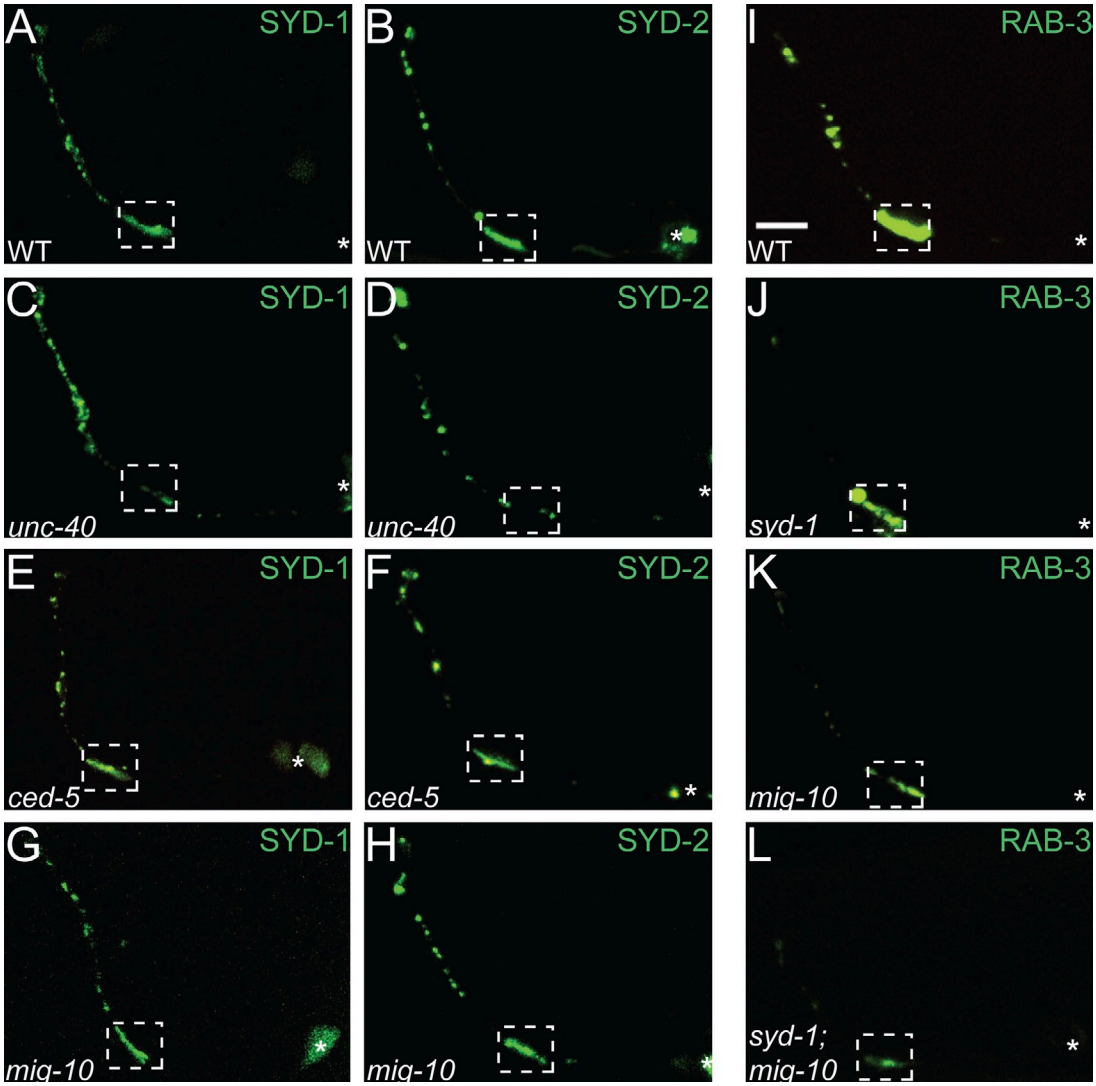

Figure 6. **CED-5 and MIG-10 are not required for the presynaptic localization of active zone proteins.** (A–H) Localization of active zone proteins, SYD-1::GFP (A, C, E, and G) and SYD-2::GFP (B, D, F, and H) in wild type (A and B), *unc-40(e271)* (C and D), *ced-5(n1812)* (E and F), and *mig-10(ct41)* (G and H) mutant animals. Note that in *unc-40* mutants SYD-1::GFP and SYD-2::GFP display disrupted localization in presynaptic zones compared with wild type. However, *mig-10* and *ced-5* mutants do not display altered localization of these active zone proteins as compared with wild type. (I–L) Distribution of synaptic vesicle clusters (visualized with GFP:RAB-3) in wild type (I), *syd-1(ju82)* (J), *mig-10(ct41)* (K), and *syd-1(ju82);mig-10(ct41)* (L) mutants. Although both *syd-1* and *mig-10* mutants display a high penetrance defect in synaptic vesicle distribution, *syd-1;mig-10* double mutants display an enhanced expressivity of the mutant phenotype. In all images, the dashed box encloses Zone 2 and asterisk represents location of the cell body. Bar, 5 µm.

(Burkel et al., 2007). In wild-type animals, we observed that F-actin was enriched in the presynaptic regions of AIY ($n = 66$; Fig. 7, B and C). We then examined the requirement of UNC-6 and its receptor, UNC-40, in presynaptic F-actin accumulation by visualizing the UtrCH::GFP marker in *unc-6(ev400)* and *unc-40(e271)* mutants (Fig. 7, D and E). We observed a statistically significant reduction of F-actin accumulation in presynaptic regions in *unc-6(ev400)* and *unc-40(e271)* mutants, consistent with a role for Netrin in regulating the organization of actin in presynaptic regions ($n = 11$, $n = 17$, respectively; Fig. 7 B).

To examine if Rac GTPases and MIG-10 were also required for F-actin accumulation at presynaptic sites, we visualized the UtrCH::GFP marker in *ced-10(n3246)* and *mig-10(ct41)* mutants (unpublished data and Fig. 7 F, respectively). Similar to *unc-6(ev400)* and *unc-40(e271)* mutants, *ced-10(n3246)* and *mig-10(ct41)* mutants displayed statistically significant reductions of F-actin accumulation at presynaptic sites ($n = 25$, $n = 45$, respectively; Fig. 7 B). These data indicate that Netrin, Rac GTPases, and MIG-10 are required for F-actin accumulation in presynaptic regions. In addition, we observed that MIG-10 partially colocalized with F-actin at presynaptic regions (Fig. 7, G–I). Therefore, our data indicate that CED-10 and MIG-10 are required downstream of Netrin to organize the actin cytoskeleton and instruct synaptic vesicle clustering in AIY presynaptic regions.

Discussion

Studies in *C. elegans*, *Drosophila*, and vertebrates have demonstrated that Netrin plays a conserved role in instructing synapse formation (Winberg et al., 1998; Colón-Ramos et al., 2007;

Published March 26, 2012

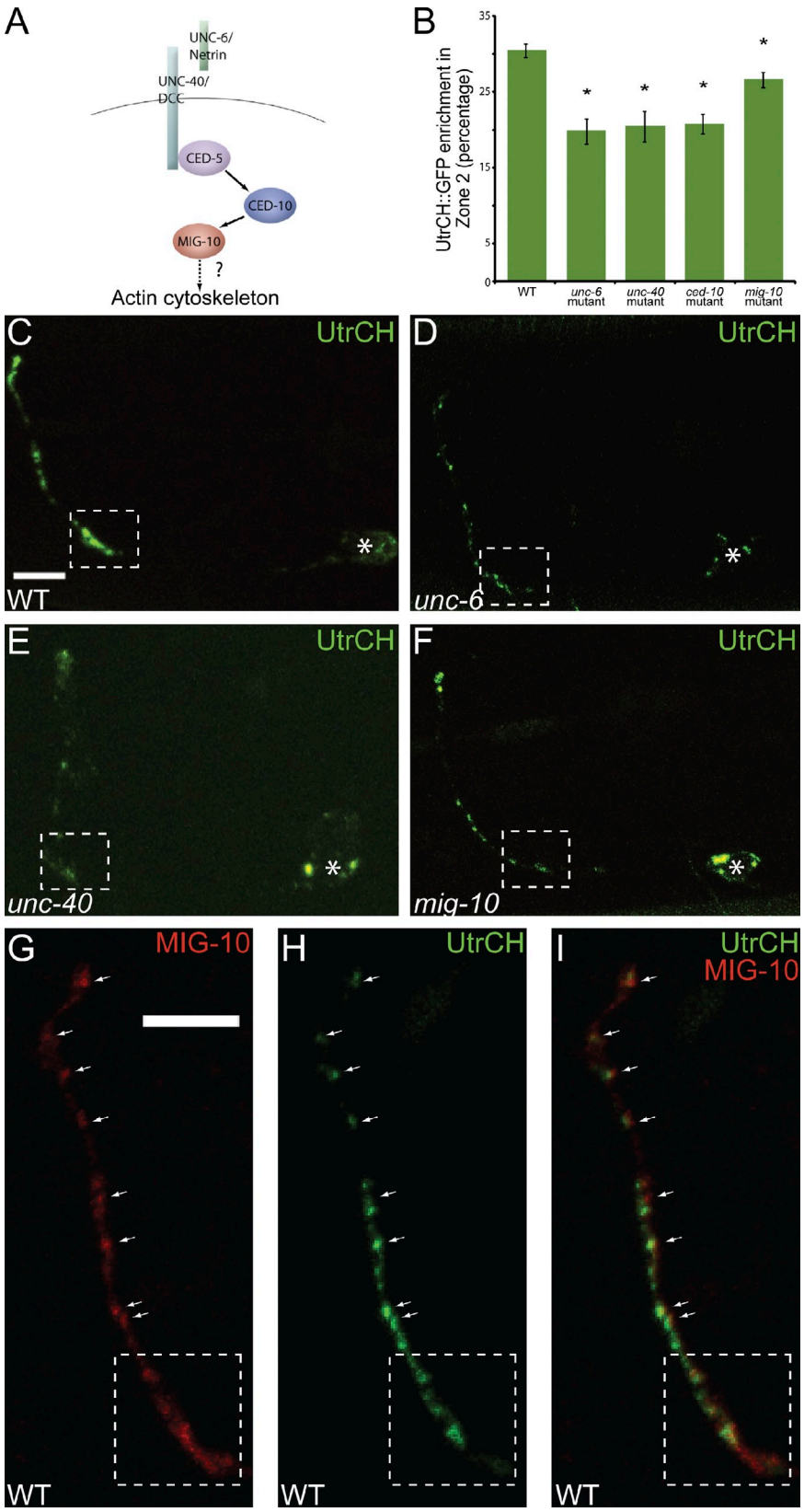

Figure 7. **MIG-10 is required for F-actin organization in presynaptic regions.** (A) Schematic of the examined pathway. (B) Quantification of the distribution of F-actin, as visualized by the UtrCH::GFP probe, in AIY Zone 2 region in wild type (n = 66), *unc-6(ev400)* (n = 11), *unc-40(e271)* (n = 17), *ced-10(n3246)* (n = 25), and *mig-10(ct41)* (n = 45) mutants. *, $P < 0.05$ between mutants and wild type by Fischer individual and Tukey simultaneous confidence intervals. Error bars represent SEM. (C–F) Confocal micrographs of animals expressing the F-actin probe, UtrCH::GFP, cell-specifically in AIY in wild type (C), *unc-6(ev400)* (D), *unc-40(e271)* (E), and *mig-10(ct41)* (F) mutant animals. Note that F-actin is disorganized in *unc-6 (ev400)*, *unc-40(e271)*, *mig-10(ct41)* mutants and that there is decreased F-actin accumulation in Zone 2 compared with wild type. Bar (C–F), 5 µm. (G–I) Confocal micrographs of Zones 2 and 3 of a transgenic animal expressing MIG-10::mCh (G) and UtrCH::GFP (H) cell-specifically in AIY. Merge in panel I. Synaptic regions are expanded in these images to allow evaluation of partial colocalization of the two proteins (arrows). In all images, the dashed box encloses Zone 2 and asterisk represents location of the cell body. Bar (G–I), 5 µm.

Poon et al., 2008; Manitt et al., 2009; Xu et al., 2010; Park et al., 2011). How Netrin instructs synapse formation and how these mechanisms relate to Netrin's canonical guidance role are not understood. Here we identify the molecular mechanisms by which Netrin instructs synaptic vesicle clustering in the *C. elegans* AIY interneuron. Our data indicate that Netrin instructs synaptic vesicle clustering through the GEF CED-5, the GTPase CED-10, and cytoplasmic adapter molecule MIG-10. These three molecules

Published March 26, 2012

are required for Netrin-mediated cell migration and axon guidance in other neurons (Manser and Wood, 1990; Lundquist et al., 2001; Gitai et al., 2003; Adler et al., 2006; Chang et al., 2006; Quinn et al., 2008). In AIY, these molecules are instead required for synaptic vesicle clustering downstream of Netrin. Although our cell biological study was focused on the AIY interneuron, the identified pathways are well conserved throughout evolution. Therefore, we hypothesize the mechanisms reported here will also instruct vesicle clustering in other cells and organisms where Netrin and DCC direct synapse formation.

Interestingly, we find that these molecules are dispensable for instructing the localization of active zone proteins, which suggests a genetic separation of these signaling pathways downstream of UNC-40. Our data are consistent with observations from other genetic studies. For instance, a genetic study in *C. elegans* GABAergic neurons resulted in the identification of mutants required for the localization of active zone protein SYD-2, but not for the localization of synaptic vesicle protein SNB-1 (Yeh et al., 2005). Moreover, in *Drosophila*, ghost boutons, which are not in direct contact with postsynaptic partners, lack active zone proteins yet contain synaptic vesicles (Ataman et al., 2006). Therefore, in some developmental contexts, including AIY, active zone assembly and synaptic vesicle localization are genetically separable events. It should be noted, however, that we do observe that active zone proteins are required for the clustering of synaptic vesicles in AIY. Double-mutant analyses between *syd-1(ju82);mig-10(ct41)* suggest that these two molecules act in parallel in vesicle clustering. Together, our findings indicate that a single receptor, UNC-40, can instruct vesicle clustering by simultaneously activating a Rac GTPase pathway and instructing the localization of active zone proteins.

We show that synaptic vesicle clustering at the synaptogenic site results from the asymmetric localization of a signaling module in response to Netrin. We find that the asymmetric organization of the signaling molecules starts with the localization of the Netrin receptor UNC-40. Glia-derived Netrin modulates the asymmetric accumulation of UNC-40 through an interaction with the UNC-40 ectodomain. UNC-40 then directs synaptic vesicle clustering at the Netrin-specified coordinate through the UNC-40 intracellular domain. We found that CED-5 localizes to presynaptic sites in response to Netrin and is required for synaptic vesicle clustering in AIY. Our data also suggest that CED-5 signals through the Rac GTPase CED-10 to instruct synaptic vesicle clustering. In many disparate neurodevelopmental events, Racs modulate the asymmetric reorganization of the actin cytoskeleton in response to extracellular cues (de Curtis, 2008; Miyamoto and Yamauchi, 2010). In synapse formation, the role of Racs is best understood at postsynaptic spines (de Curtis, 2008). We now find that at presynaptic sites, Racs can also instruct asymmetric organization of the actin cytoskeleton and direct synaptogenesis in response to Netrin.

The pathway we report here is required for the correct organization of the actin cytoskeleton in response to Netrin. Thus, Netrin-mediated cytoskeletal reorganization underlies both axon guidance and synaptogenesis. Surprisingly little is known regarding the role of actin during presynaptic assembly (Dillon and Goda, 2005; Cingolani and Goda, 2008; Geraldo and Gordon-Weeks, 2009). Tissue culture studies have demonstrated that F-actin is essential for the early development of presynaptic sites (Zhang and Benson, 2001; Dillon and Goda, 2005; Cingolani and Goda, 2008). Given our data and these findings, we propose that Netrin instructs synaptic vesicle clustering by organizing F-actin in presynaptic regions. Therefore, a signaling module used in other cells during axon guidance is synaptically localized in AIY to instruct synaptic vesicle clustering.

The development of the nervous system is orchestrated with a limited number of molecular cues. As we learn more about these molecular factors, we are discovering that distinct neurodevelopmental events share common signaling molecules. Our findings indicate that Netrin activates similar pathways while instructing guidance and synaptic vesicle clustering. We find that while directing synaptic vesicle clustering, UNC-40 and its downstream signaling module are subcellularly localized to presynaptic regions of AIY. Our work provides evidence that in vivo neurodevelopmental outcomes may be differentially instructed between cells, not only through novel intracellular signaling pathways, but also through the directed asymmetric localization of known signaling complexes.

Materials and methods

Strains and genetics

Worms were raised on NGM plates at 20°C using OP50 *Escherichia coli* as a food source. N2 Bristol was used as the wild-type reference strain. The following mutant strains were obtained through the *Caenorhabditis* Genetics Center: *ced-10(n3246)IV, unc-40(e271)I, unc-6(ev400)X, mig-10 (ct41)III, ced-5(n1812)IV, unc-73((e936)I, mig-2(mu28)X, rac-2(ok326)IV, ced-10(n1993)IV, syd-1(ju82)II,* and *unc-115(ky275)X*. The alleles *ced-5 (tm1949)IV* and *ced-5(tm1950)* were kindly provided by the Mitani laboratory of the Tokyo Women's Medical University School of Medicine (Tokyo, Japan). The *ced-5(n1812);ced-10(n1993)* parent strain for the double mutant was kindly provided by the Horvitz laboratory of the Massachusetts Institute of Technology (Cambridge, MA).

The *unc-40(e271)* mutation is a null allele. The nucleotide polymorphism is c7968t and results in a R824* (Arg to opal stop) in the ectodomain (Roy, P., personal communication).

Molecular biology and transgenic lines

Expression clones were made in the pSM vector (Shen and Bargmann, 2003). The plasmids and transgenic strains (0.5–30 ng/µl) were generated using standard techniques and coinjected with markers *Punc122::gfp* or *Punc122::dsRed* (15–30 ng/µl): *wyIs45* [Pttx3::gfp::rab3], *wyEx1149* [Pttx3::unc40::gfp], *wyEx523* [Pttx3::unc40 ectodomain::mch], *wyEx540* [Pttx3::unc40 endodomain::mch], *wyEx1697* [Punc40::unc40 ectodomain], *wyEx650* [Punc40::unc40], *olaEx586* [Pttx3::gfp, Phlh17::mch], *olaEx738* [Pttx3::gfp, Phlh17::mch], *olaEx745* [Punc40::unc40minigene::ced5], *olaEx581* [Pttx3::ced5::gfp], *olaEx135* [Pttx3::rfp, Pglr3::rfp, Fosmid WRM 066dB08], *olaEx324* [Pttx3::mig10b::gfp], *olaEx294* [Pttx3::UtrCH::gfp], *olaEx410* [Pttx3::mig10b::mCh, Pttx3::UtrCh::gfp], *olaEx602* [Pmig10b::gfp, Pttx3::rfp], *olaEx866* [Pttx3::snb-1::yfp, Pttx3::mCh::rab3], *olaEx915* [Pttx3::sng1::yfp, Pttx3::mCh::rab3], *wyIs93* [Pglr3::mCh::rab3, Pglr3::glr1::gfp], *wyEx1826* [Pttx3::syd2::gfp], and *olaEx297* [Pttx3::syd1::gfp].

Detailed subcloning information will be provided upon request. MIG-10B cDNA was isolated by PCR from cDNA collected from a mixed stage population. CED-5, MIG-2, and RAC-2 cDNA were obtained by the same methods. The UNC-40:CED-5 chimera fusion protein was constructed with CED-5 cDNA fused in-frame to the C terminus of the UNC-40 minigene (Colón-Ramos et al., 2007), driven by the endogenous UNC-40 promoter.

Fluorescence microscopy and confocal imaging

Images of fluorescently tagged fusion proteins (eGFP, GFP, YFP, and mCherry with excitation wavelengths of 488 and 561 nm) were captured at room temperature in live *C. elegans* using a 60x CFI Plan Apochromat VC, NA 1.4, oil objective (Nikon) on an UltraView VoX spinning-disc confocal microscope (PerkinElmer) on a stand (Ti-E; Nikon) with an EM-CCD camera

(model C9100-50; Hamamatsu Photonics). Images were acquired and processed with Volocity software (PerkinElmer). All images are maximal projections ("Extended Focus" in Volocity). Final processing of images, including rotation and cropping, was performed with Adobe Photoshop CS4 (Adobe Systems, Inc.). Any quantifications were performed on maximal projections of raw data. Worms were immobilized using 10 mM levamisole (Sigma-Aldrich) and oriented anterior to the left and dorsal up.

Mosaic analysis

Mosaic analysis was conducted on *mig-10(ct41)* animals by expressing unstable transgenes with a *mig-10* rescuing construct and cytoplasmic markers in RIA and AIY (*olaEx135*). Animals were inspected for retention of the transgene and rescue of AIY presynaptic patterning using a microscope (model DM5000 B; Leica). We conducted mosaic analysis for AIY presynaptic patterning by scoring *mig-10(ct41)* animals for rescue of synaptic vesicle distribution in AIY, as defined by an enrichment of synaptic vesicles in Zone 2 and discrete synaptic vesicle clusters in Zone 3. Array retention was tracked in AIY and RIA with cytoplasmic RFP (Yochem and Herman, 2003; Colón-Ramos et al., 2007; Herman, 2007).

Quantification

Quantification of the axon guidance or cell migration phenotype in AIY was conducted as described previously (Colón-Ramos et al., 2007). In brief, 3D reconstructions of confocal micrographs were closely examined and scored for the cell migration of the AIY cell body to the retrovesicular ganglion and the three navigational decisions AIY makes as it traverses the ventral nerve cord and the nerve ring: (1) anterior projection through the ventral nerve cord, (2) dorsal turn at the nerve ring, and (3) circumnavigation of the nerve ring until the AIY neurite contacts the sister AIY at the dorsal midline. Significance was determined using a two-tailed Fisher's exact test.

Quantification of the distribution of GFP::RAB-3 in AIY was completed by measuring average fluorescence intensity over the Zone 2 region in confocal micrographs. Fluorescence intensity was measured using the line scan function of ImageJ (National Institutes of Health, Bethesda, MD) and tracing the AIY process. To measure the average fluorescence intensity in Zone 2, Zone 2 was morphologically defined in adult animals as the region of the AIY process which encompasses the dorsal turn as the process exits the anterior ventral nerve cord and enters the nerve ring (~5 µm; boxed in all figures; Colón-Ramos et al., 2007). This anatomical definition of Zone 2 was informed by the reconstructions of EM micrographs in White et al. (1986). In wild-type animals AIY forms synapses with RIA only in the Zone 2 region, as determined by reconstructions of EM micrographs. In addition, in wild-type animals the AIY axon width is roughly four times larger in Zone 2 than in Zone 3 (White et al., 1986; Colón-Ramos et al., 2007). Total fluorescence intensity in this region was divided by the exact length of the measured Zone 2, yielding the average fluorescence intensity over the Zone 2 region. To determine average total AIY fluorescence intensity of GFP::RAB-3, Zone 2 average fluorescence was added to Zone 3 average fluorescence. To determine the average fluorescence intensity of GFP::RAB-3 in Zone 3, Zone 3 was morphologically defined as the region of the AIY neurite immediately dorsal to the Zone 2 region extending to the end of the dorsal midline. Total fluorescence intensity in this region was divided by the exact length of the measured Zone 3, yielding the average fluorescence intensity over Zone 3.

To quantify the enrichment of MIG-10::GFP and UtrCH::GFP in AIY, we first identified extrachromosomal transgenic lines that displayed stable expression of MIG-10::GFP or UtrCH::GFP (*olaEx324* and *olaEx294*, respectively). To ensure consistency across experiments, the same extrachromosomal line for each construct was then crossed into the specified mutant backgrounds. Quantification was completed by using the line scan function of ImageJ and tracing the AIY process. Quantifications were performed blindly, without knowledge of the genotype. The fluorescence intensity in Zones 2 and 3 were determined as described above. Total fluorescence intensity of the Zone 2 region was divided by total fluorescence intensity of both Zones 2 and 3, yielding MIG-10::GFP or UtrCH::GFP enrichment in Zone 2.

Statistical analyses

Statistical significance for categorical data was determined using Fischer's exact test. Error bars for categorical data were calculated using 95% confidence intervals. For Figs. 2 H, 3 O, 4 G, 5 E, and 7 B, statistical significance for continuous data was determined using one-way ANOVA with post-hoc analysis by Fischer individual and Tukey simultaneous confidence intervals using Minitab16 software. Error bars for continuous data were calculated using standard errors of the mean.

Online supplemental material

Fig. S1 and Fig. S2 display colocalization of mCh::RAB-3 and SNB-1::YFP or SNG-1::YFP, respectively, in relevant mutant backgrounds. Fig. S3 demonstrates that UNC-40 localization to presynaptic regions is dependent on UNC-6. Fig. S4 depicts AIY cell migration and axon guidance in relevant mutant backgrounds. Fig. S5 shows RIA cell migration, guidance, and pre- and postsynaptic localization in relevant mutant backgrounds. Online supplemental material is available at http://www.jcb.org/cgi/content/full/jcb.201110127/DC1.

We thank D. Chao, K. Spilker, M. Margeta, W. Bement, the *Caenorhabditis* Genetic Center, and the Japanese National BioResource Project (NBPR) for strains and reagents. We thank Z. Altun (www.wormatlas.org) for diagrams used in the figures. We thank in particular K. Shen and J. Nelson for helpful discussions and generous sharing of advice and reagents. We also thank C. Gao and G. Chatterjee for technical assistance and M. Hammarlund, S. Margolis, C. Smith, M. Hurwitz, and members of the Colón-Ramos laboratory for thoughtful comments on the manuscript.

This work was funded by the following grants to D. Colón-Ramos: R00 NS057931 from the National Institutes of Health (NIH), a fellowship from the Klingenstein Foundation, the Alfred P. Sloan Foundation, and a March of Dimes research grant. A. Stavoe was supported by Cellular and Molecular Biology Training grant T32-GM007223 from the NIH.

Submitted: 28 October 2011
Accepted: 29 February 2012

References

Adler, C.E., R.D. Fetter, and C.I. Bargmann. 2006. UNC-6/Netrin induces neuronal asymmetry and defines the site of axon formation. *Nat. Neurosci.* 9:511–518. http://dx.doi.org/10.1038/nn1666

Altun-Gultekin, Z., Y. Andachi, E.L. Tsalik, D. Pilgrim, Y. Kohara, and O. Hobert. 2001. A regulatory cascade of three homeobox genes, ceh-10, ttx-3 and ceh-23, controls cell fate specification of a defined interneuron class in *C. elegans*. *Development*. 128:1951–1969.

Ataman, B., J. Ashley, D. Gorczyca, M. Gorczyca, D. Mathew, C. Wichmann, S.J. Sigrist, and V. Budnik. 2006. Nuclear trafficking of *Drosophila* Frizzled-2 during synapse development requires the PDZ protein dGRIP. *Proc. Natl. Acad. Sci. USA*. 103:7841–7846. http://dx.doi.org/10.1073/pnas.0600387103

Briançon-Marjollet, A., A. Ghogha, H. Nawabi, I. Triki, C. Auziol, S. Fromont, C. Piché, H. Enslen, K. Chebli, J.F. Cloutier, et al. 2008. Trio mediates netrin-1-induced Rac1 activation in axon outgrowth and guidance. *Mol. Cell. Biol.* 28:2314–2323. http://dx.doi.org/10.1128/MCB.00998-07

Burkel, B.M., G. von Dassow, and W.M. Bement. 2007. Versatile fluorescent probes for actin filaments based on the actin-binding domain of utrophin. *Cell Motil. Cytoskeleton*. 64:822–832. http://dx.doi.org/10.1002/cm.20226

Chang, C., C.E. Adler, M. Krause, S.G. Clark, F.B. Gertler, M. Tessier-Lavigne, and C.I. Bargmann. 2006. MIG-10/lamellipodin and AGE-1/PI3K promote axon guidance and outgrowth in response to slit and netrin. *Curr. Biol.* 16:854–862. http://dx.doi.org/10.1016/j.cub.2006.03.083

Chen, S.Y., and H.J. Cheng. 2009. Functions of axon guidance molecules in synapse formation. *Curr. Opin. Neurobiol.* 19:471–478. http://dx.doi.org/10.1016/j.conb.2009.09.005

Cingolani, L.A., and Y. Goda. 2008. Actin in action: the interplay between the actin cytoskeleton and synaptic efficacy. *Nat. Rev. Neurosci.* 9:344–356. http://dx.doi.org/10.1038/nrn2373

Colicos, M.A., B.E. Collins, M.J. Sailor, and Y. Goda. 2001. Remodeling of synaptic actin induced by photoconductive stimulation. *Cell*. 107:605–616. http://dx.doi.org/10.1016/S0092-8674(01)00579-7

Colón-Ramos, D.A., M.A. Margeta, and K. Shen. 2007. Glia promote local synaptogenesis through UNC-6 (netrin) signaling in *C. elegans*. *Science*. 318:103–106. http://dx.doi.org/10.1126/science.1143762

Dai, Y., H. Taru, S.L. Deken, B. Grill, B. Ackley, M.L. Nonet, and Y.S. Jin. 2006. SYD-2 Liprin-alpha organizes presynaptic active zone formation through ELKS. *Nat. Neurosci.* 9:1479–1487. http://dx.doi.org/10.1038/nn1808

Davis, E.K., Y. Zou, and A. Ghosh. 2008. Wnts acting through canonical and noncanonical signaling pathways exert opposite effects on hippocampal synapse formation. *Neural Dev.* 3:32. http://dx.doi.org/10.1186/1749-8104-3-32

de Curtis, I. 2008. Functions of Rac GTPases during neuronal development. *Dev. Neurosci.* 30:47–58. http://dx.doi.org/10.1159/000109851

Dillon, C., and Y. Goda. 2005. The actin cytoskeleton: integrating form and function at the synapse. *Annu. Rev. Neurosci.* 28:25–55. http://dx.doi.org/10.1146/annurev.neuro.28.061604.135757

Forsthoefel, D.J., E.C. Liebl, P.A. Kolodziej, and M.A. Seeger. 2005. The Abelson tyrosine kinase, the Trio GEF and Enabled interact with the Netrin receptor Frazzled in *Drosophila*. *Development*. 132:1983–1994. http://dx.doi.org/10.1242/dev.01736

Geraldo, S., and P.R. Gordon-Weeks. 2009. Cytoskeletal dynamics in growth-cone steering. *J. Cell Sci.* 122:3595–3604. http://dx.doi.org/10.1242/jcs.042309

Gitai, Z., T.W. Yu, E.A. Lundquist, M. Tessier-Lavigne, and C.I. Bargmann. 2003. The netrin receptor UNC-40/DCC stimulates axon attraction and outgrowth through enabled and, in parallel, Rac and UNC-115/AbLIM. *Neuron*. 37:53–65. http://dx.doi.org/10.1016/S0896-6273(02)01149-2

Hallam, S.J., A. Goncharov, J. McEwen, R. Baran, and Y. Jin. 2002. SYD-1, a presynaptic protein with PDZ, C2 and rhoGAP-like domains, specifies axon identity in *C. elegans*. *Nat. Neurosci.* 5:1137–1146. http://dx.doi.org/10.1038/nn959

Hedgecock, E.M., J.G. Culotti, and D.H. Hall. 1990. The unc-5, unc-6, and unc-40 genes guide circumferential migrations of pioneer axons and mesodermal cells on the epidermis in *C. elegans*. *Neuron*. 4:61–85. http://dx.doi.org/10.1016/0896-6273(90)90444-K

Herman, R.K. 2007. Mosaic analysis in the nematode *Caenorhabditis elegans*. *J. Neurogenet.* 21:219–242. http://dx.doi.org/10.1080/01677060701693446

Honigberg, L., and C. Kenyon. 2000. Establishment of left/right asymmetry in neuroblast migration by UNC-40/DCC, UNC-73/Trio and DPY-19 proteins in *C. elegans*. *Development*. 127:4655–4668.

Inaki, M., S. Yoshikawa, J.B. Thomas, H. Aburatani, and A. Nose. 2007. Wnt4 is a local repulsive cue that determines synaptic target specificity. *Curr. Biol.* 17:1574–1579. http://dx.doi.org/10.1016/j.cub.2007.08.013

Ishii, N., W.G. Wadsworth, B.D. Stern, J.G. Culotti, and E.M. Hedgecock. 1992. UNC-6, a laminin-related protein, guides cell and pioneer axon migrations in *C. elegans*. *Neuron*. 9:873–881. http://dx.doi.org/10.1016/0896-6273(92)90240-E

Jin, Y., and C.C. Garner. 2008. Molecular mechanisms of presynaptic differentiation. *Annu. Rev. Cell Dev. Biol.* 24:237–262. http://dx.doi.org/10.1146/annurev.cellbio.23.090506.123417

Kiyokawa, E., Y. Hashimoto, S. Kobayashi, H. Sugimura, T. Kurata, and M. Matsuda. 1998. Activation of Rac1 by a Crk SH3-binding protein, DOCK180. *Gene Dev.* 12:3331–3336. http://dx.doi.org/ 10.1101/gad.12.21.3331

Klassen, M.P., and K. Shen. 2007. Wnt signaling positions neuromuscular connectivity by inhibiting synapse formation in *C. elegans*. *Cell*. 130:704–716. http://dx.doi.org/10.1016/j.cell.2007.06.046

Li, X., M. Meriane, I. Triki, M. Shekarabi, T.E. Kennedy, L. Larose, and N. Lamarche-Vane. 2002a. The adaptor protein Nck-1 couples the netrin-1 receptor DCC (deleted in colorectal cancer) to the activation of the small GTPase Rac1 through an atypical mechanism. *J. Biol. Chem.* 277:37788–37797. http://dx.doi.org/10.1074/jbc.M205428200

Li, X., E. Saint-Cyr-Proulx, K. Aktories, and N. Lamarche-Vane. 2002b. Rac1 and Cdc42 but not RhoA or Rho kinase activities are required for neurite outgrowth induced by the Netrin-1 receptor DCC (deleted in colorectal cancer) in N1E-115 neuroblastoma cells. *J. Biol. Chem.* 277:15207–15214. http://dx.doi.org/10.1074/jbc.M109913200

Li, X., X. Gao, G. Liu, W. Xiong, J. Wu, and Y. Rao. 2008. Netrin signal transduction and the guanine nucleotide exchange factor DOCK180 in attractive signaling. *Nat. Neurosci.* 11:28–35. http://dx.doi.org/10.1038/nn2022

Livesey, F.J. 1999. Netrins and netrin receptors. *Cell. Mol. Life Sci.* 56:62–68. http://dx.doi.org/10.1007/s000180050006

Lucido, A.L., F. Suarez Sanchez, P. Thostrup, A.V. Kwiatkowski, S. Leal-Ortiz, G. Gopalakrishnan, D. Liazoghli, W. Belkaid, R.B. Lennox, P. Grutter, et al. 2009. Rapid assembly of functional presynaptic boutons triggered by adhesive contacts. *J. Neurosci.* 29:12449–12466. http://dx.doi.org/10.1523/JNEUROSCI.1381-09.2009

Lundquist, E.A., R.K. Herman, J.E. Shaw, and C.I. Bargmann. 1998. UNC-115, a conserved protein with predicted LIM and actin-binding domains, mediates axon guidance in *C. elegans*. *Neuron*. 21:385–392. http://dx.doi.org/10.1016/S0896-6273(00)80547-4

Lundquist, E.A., P.W. Reddien, E. Hartwieg, H.R. Horvitz, and C.I. Bargmann. 2001. Three *C. elegans* Rac proteins and several alternative Rac regulators control axon guidance, cell migration and apoptotic cell phagocytosis. *Development*. 128:4475–4488.

Manitt, C., A.M. Nikolakopoulou, D.R. Almario, S.A. Nguyen, and S. Cohen-Cory. 2009. Netrin participates in the development of retinotectal synaptic connectivity by modulating axon arborization and synapse formation in the developing brain. *J. Neurosci.* 29:11065–11077. http://dx.doi.org/10.1523/JNEUROSCI.0947-09.2009

Manser, J., and W.B. Wood. 1990. Mutations affecting embryonic cell migrations in *Caenorhabditis elegans*. *Dev. Genet.* 11:49–64. http://dx.doi.org/10.1002/dvg.1020110107

Manser, J., C. Roonprapunt, and B. Margolis. 1997. *C. elegans* cell migration gene mig-10 shares similarities with a family of SH2 domain proteins and acts cell nonautonomously in excretory canal development. *Dev. Biol.* 184:150–164. http://dx.doi.org/10.1006/dbio.1997.8516

Matteoli, M., K. Takei, R. Cameron, P. Hurlbut, P.A. Johnston, T.C. Südhof, R. Jahn, and P. De Camilli. 1991. Association of Rab3A with synaptic vesicles at late stages of the secretory pathway. *J. Cell Biol.* 115:625–633. http://dx.doi.org/10.1083/jcb.115.3.625

Miech, C., H.U. Pauer, X. He, and T.L. Schwarz. 2008. Presynaptic local signaling by a canonical wingless pathway regulates development of the *Drosophila* neuromuscular junction. *J. Neurosci.* 28:10875–10884. http://dx.doi.org/10.1523/JNEUROSCI.0164-08.2008

Miyamoto, Y., and J. Yamauchi. 2010. Cellular signaling of Dock family proteins in neural function. *Cell. Signal.* 22:175–182. http://dx.doi.org/10.1016/j.cellsig.2009.09.036

Nolan, K.M., K. Barrett, Y. Lu, K.Q. Hu, S. Vincent, and J. Settleman. 1998. Myoblast city, the *Drosophila* homolog of DOCK180/CED-5, is required in a Rac signaling pathway utilized for multiple developmental processes. *Genes Dev.* 12:3337–3342. http://dx.doi.org/10.1101/gad.12.21.3337

Nonet, M.L. 1999. Visualization of synaptic specializations in live *C. elegans* with synaptic vesicle protein-GFP fusions. *J. Neurosci. Methods*. 89:33–40. http://dx.doi.org/10.1016/S0165-0270(99)00031-X

Park, J., P.L. Knezevich, W. Wung, S.N. O'Hanlon, A. Goyal, K.L. Benedetti, B.J. Barsi-Rhyne, M. Raman, N. Mock, M. Bremer, and M.K. Vanhoven. 2011. A conserved juxtacrine signal regulates synaptic partner recognition in *Caenorhabditis elegans*. *Neural Dev.* 6:28. http://dx.doi.org/10.1186/1749-8104-6-28

Patel, M.R., E.K. Lehrman, V.Y. Poon, J.G. Crump, M. Zhen, C.I. Bargmann, and K. Shen. 2006. Hierarchical assembly of presynaptic components in defined *C. elegans* synapses. *Nat. Neurosci.* 9:1488–1498. http://dx.doi.org/10.1038/nn1806

Poon, V.Y., M.P. Klassen, and K. Shen. 2008. UNC-6/netrin and its receptor UNC-5 locally exclude presynaptic components from dendrites. *Nature*. 455:669–673. http://dx.doi.org/10.1038/nature07291

Quinn, C.C., and W.G. Wadsworth. 2008. Axon guidance: asymmetric signaling orients polarized outgrowth. *Trends Cell Biol.* 18:597–603. http://dx.doi.org/10.1016/j.tcb.2008.09.005

Quinn, C.C., D.S. Pfeil, and W.G. Wadsworth. 2008. CED-10/Rac1 mediates axon guidance by regulating the asymmetric distribution of MIG-10/lamellipodin. *Curr. Biol.* 18:808–813. http://dx.doi.org/10.1016/j.cub.2008.04.050

Reddien, P.W., and H.R. Horvitz. 2000. CED-2/Crkll and CED-10/Rac control phagocytosis and cell migration in *Caenorhabditis elegans*. *Nat. Cell Biol.* 2:131–136. http://dx.doi.org/10.1038/35004000

Round, J., and E. Stein. 2007. Netrin signaling leading to directed growth cone steering. *Curr. Opin. Neurobiol.* 17:15–21. http://dx.doi.org/10.1016/j.conb.2007.01.003

Salinas, P.C., and Y. Zou. 2008. Wnt signaling in neural circuit assembly. *Annu. Rev. Neurosci.* 31:339–358. http://dx.doi.org/10.1146/annurev.neuro.31.060407.125649

Sankaranarayanan, S., P.P. Atluri, and T.A. Ryan. 2003. Actin has a molecular scaffolding, not propulsive, role in presynaptic function. *Nat. Neurosci.* 6:127–135. http://dx.doi.org/10.1038/nn1002

Serafini, T., T.E. Kennedy, M.J. Galko, C. Mirzayan, T.M. Jessell, and M. Tessier-Lavigne. 1994. The netrins define a family of axon outgrowth-promoting proteins homologous to *C. elegans* UNC-6. *Cell*. 78:409–424. http://dx.doi.org/10.1016/0092-8674(94)90420-0

Shekarabi, M., and T.E. Kennedy. 2002. The netrin-1 receptor DCC promotes filopodia formation and cell spreading by activating Cdc42 and Rac1. *Mol. Cell. Neurosci.* 19:1–17. http://dx.doi.org/10.1006/mcne.2001.1075

Shekarabi, M., S.W. Moore, N.X. Tritsch, S.J. Morris, J.F. Bouchard, and T.E. Kennedy. 2005. Deleted in colorectal cancer binding netrin-1 mediates cell substrate adhesion and recruits Cdc42, Rac1, Pak1, and N-WASP into an intracellular signaling complex that promotes growth cone expansion. *J. Neurosci.* 25:3132–3141. http://dx.doi.org/10.1523/JNEUROSCI.1920-04.2005

Shen, K., and C.I. Bargmann. 2003. The immunoglobulin superfamily protein SYG-1 determines the location of specific synapses in *C. elegans*. *Cell*. 112:619–630. http://dx.doi.org/10.1016/S0092-8674(03)00113-2

Shen, K., and C.W. Cowan. 2010. Guidance molecules in synapse formation and plasticity. *Cold Spring Harb. Perspect. Biol.* 2:a001842. http://dx.doi.org/10.1101/cshperspect.a001842

Struckhoff, E.C., and E.A. Lundquist. 2003. The actin-binding protein UNC-115 is an effector of Rac signaling during axon pathfinding in *C. elegans*. *Development*. 130:693–704. http://dx.doi.org/10.1242/dev.00300

Wadsworth, W.G., H. Bhatt, and E.M. Hedgecock. 1996. Neuroglia and pioneer neurons express UNC-6 to provide global and local netrin cues for guiding migrations in *C. elegans*. *Neuron*. 16:35–46. http://dx.doi.org/10.1016/S0896-6273(00)80021-5

White, J.G., E. Southgate, J.N. Thomson, and S. Brenner. 1986. The structure of the nervous system of the nematode *Caenorhabditis elegans*. *Philos. Trans. R. Soc. Lond.* 314:1–340. http://dx.doi.org/10.1098/rstb.1986.0056

Winberg, M.L., K.J. Mitchell, and C.S. Goodman. 1998. Genetic analysis of the mechanisms controlling target selection: complementary and combinatorial functions of netrins, semaphorins, and IgCAMs. *Cell*. 93:581–591. http://dx.doi.org/10.1016/S0092-8674(00)81187-3

Xu, B., J.S. Goldman, V.V. Rymar, C. Forget, P.S. Lo, S.J. Bull, E. Vereker, P.A. Barker, L.E. Trudeau, A.F. Sadikot, and T.E. Kennedy. 2010. Critical roles for the netrin receptor deleted in colorectal cancer in dopaminergic neuronal precursor migration, axon guidance, and axon arborization. *Neuroscience*. 169:932–949. http://dx.doi.org/10.1016/j.neuroscience.2010.05.025

Yeh, E., T. Kawano, R.M. Weimer, J.L. Bessereau, and M. Zhen. 2005. Identification of genes involved in synaptogenesis using a fluorescent active zone marker in *Caenorhabditis elegans*. *J. Neurosci.* 25:3833–3841. http://dx.doi.org/10.1523/JNEUROSCI.4978-04.2005

Yochem, J., and R.K. Herman. 2003. Investigating *C. elegans* development through mosaic analysis. *Development*. 130:4761–4768. http://dx.doi.org/10.1242/dev.00701

Zhang, W., and D.L. Benson. 2001. Stages of synapse development defined by dependence on F-actin. *J. Neurosci.* 21:5169–5181.

Zhang, W., and D.L. Benson. 2002. Developmentally regulated changes in cellular compartmentation and synaptic distribution of actin in hippocampal neurons. *J. Neurosci. Res.* 69:427–436. http://dx.doi.org/10.1002/jnr.10313

Zhao, H.J., and M.L. Nonet. 2001. A conserved mechanism of synaptogyrin localization. *Mol. Biol. Cell*. 12:2275–2289.

Zhen, M., and Y. Jin. 1999. The liprin protein SYD-2 regulates the differentiation of presynaptic termini in *C. elegans*. *Nature*. 401:371–375.

Ziel, J.W., E.J. Hagedorn, A. Audhya, and D.R. Sherwood. 2009. UNC-6 (netrin) orients the invasive membrane of the anchor cell in *C. elegans*. *Nat. Cell Biol.* 11:183–189. http://dx.doi.org/10.1038/ncb1825

Published March 26, 2012

Stavoe and Colón-Ramos, http://www.jcb.org/cgi/content/full/jcb.201110127/DC1

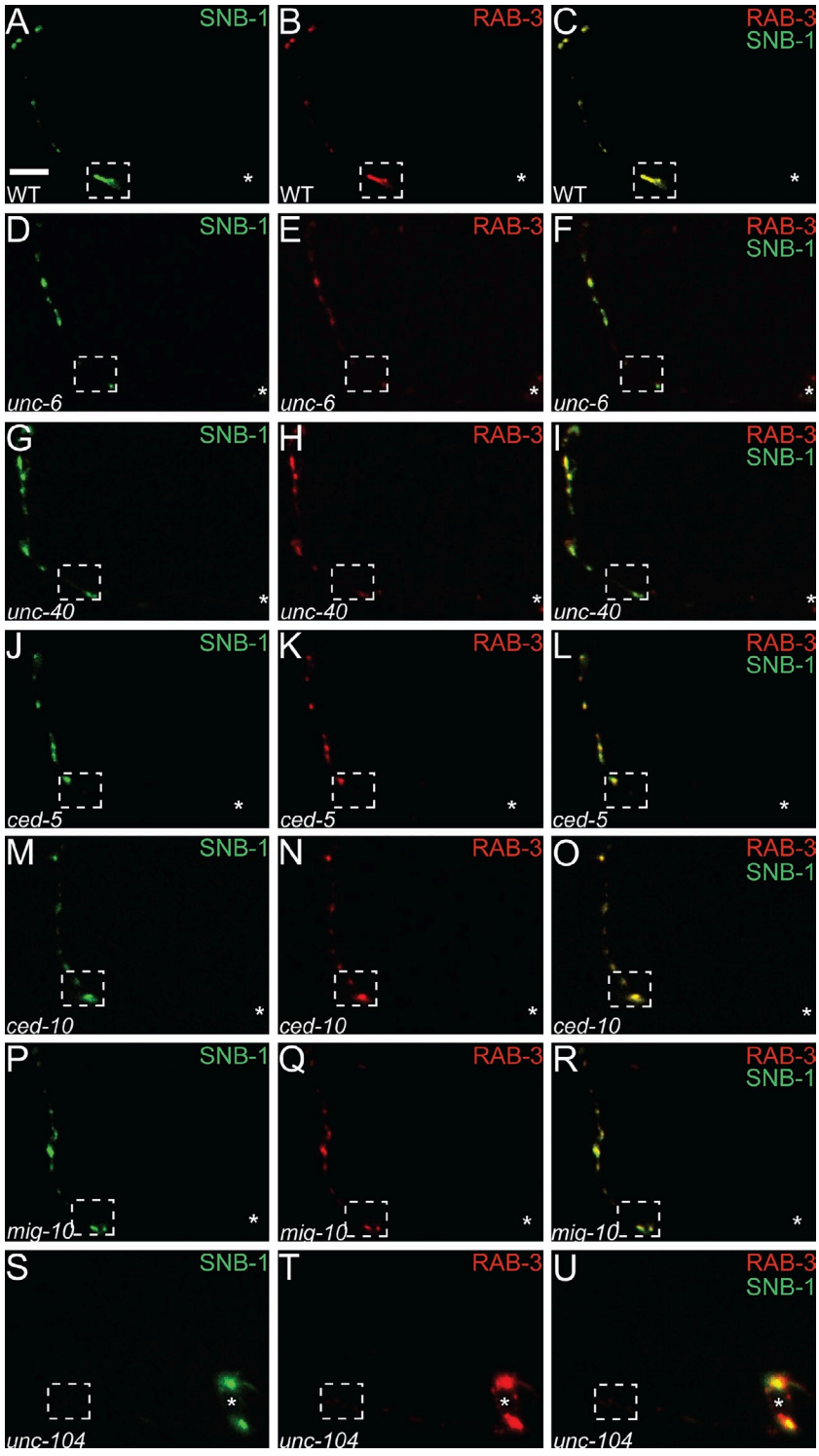

Figure S1. **Disruption of synaptobrevin-labeled AIY synaptic vesicles in pathway mutants.** (A–U) Distribution of synaptic vesicles in AIY (labeled with SNB-1::YFP and mCh::RAB-3) in wild-type (A–C), *unc-6* (D–F), *unc-40* (G–I), *ced-5* (J–L), *ced-10* (M–O), *mig-10* (P–R), and *unc-104* (S–U) mutants. The *unc-104/kinesin* mutant was examined to demonstrate that the observed fluorescence at presynaptic sites results from synaptic vesicle localization. Bar, 5 µm.

Published March 26, 2012

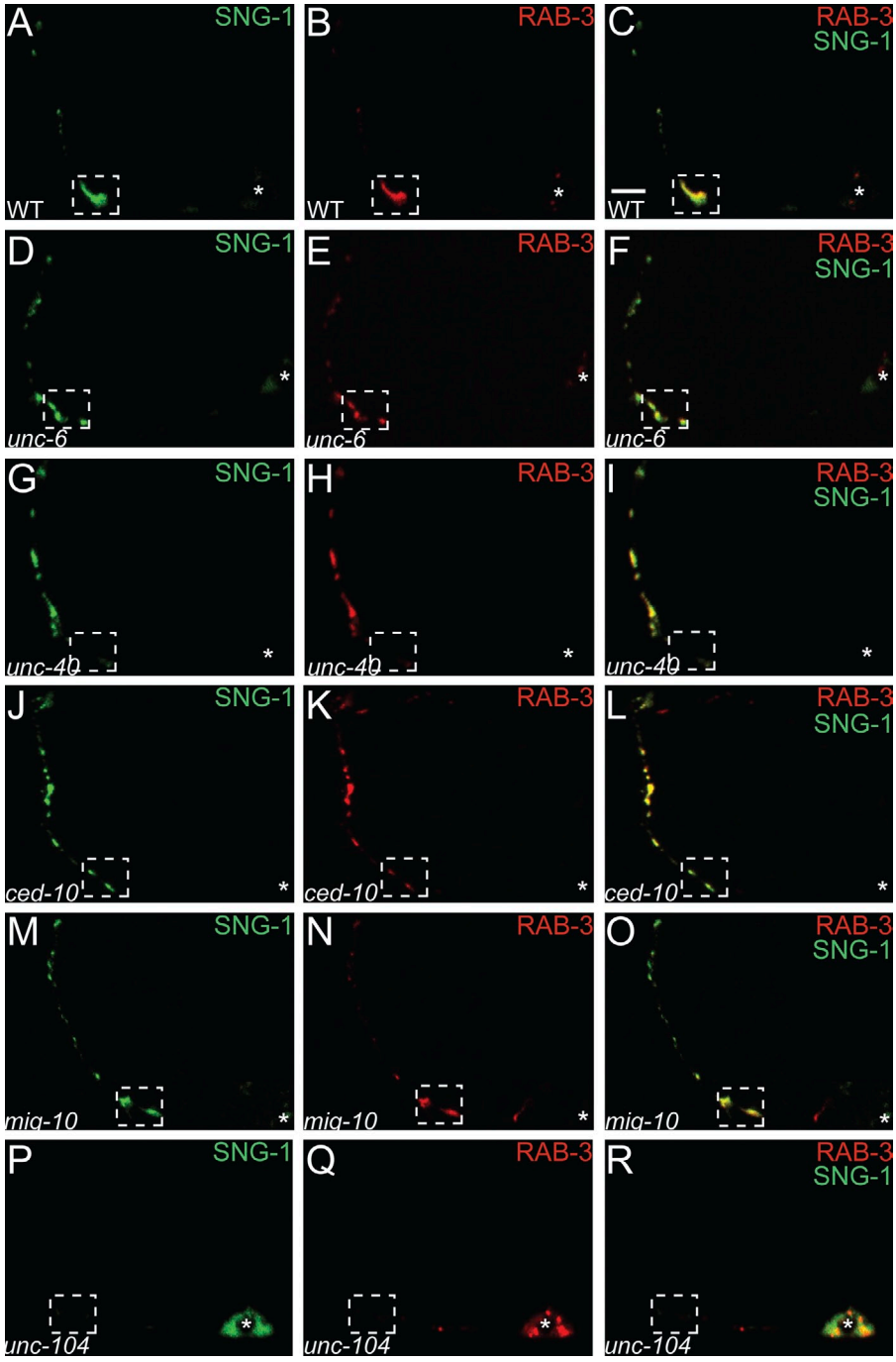

Figure S2. **Disruption of synaptogyrin-labeled AIY synaptic vesicles in pathway mutants.** (A–R) Distribution of synaptic vesicles in AIY (labeled with SNG-1::YFP and mCh::RAB-3) in wild-type (A–C), *unc-6* (D–F), *unc-40* (G–I), *ced-10* (J–L), *mig-10* (M–O), and *unc-104* (P–R) mutants. The *unc-104/kinesin* mutant was examined to demonstrate that the observed fluorescence at presynaptic sites results from synaptic vesicle localization. Bar, 5 µm.

Published March 26, 2012

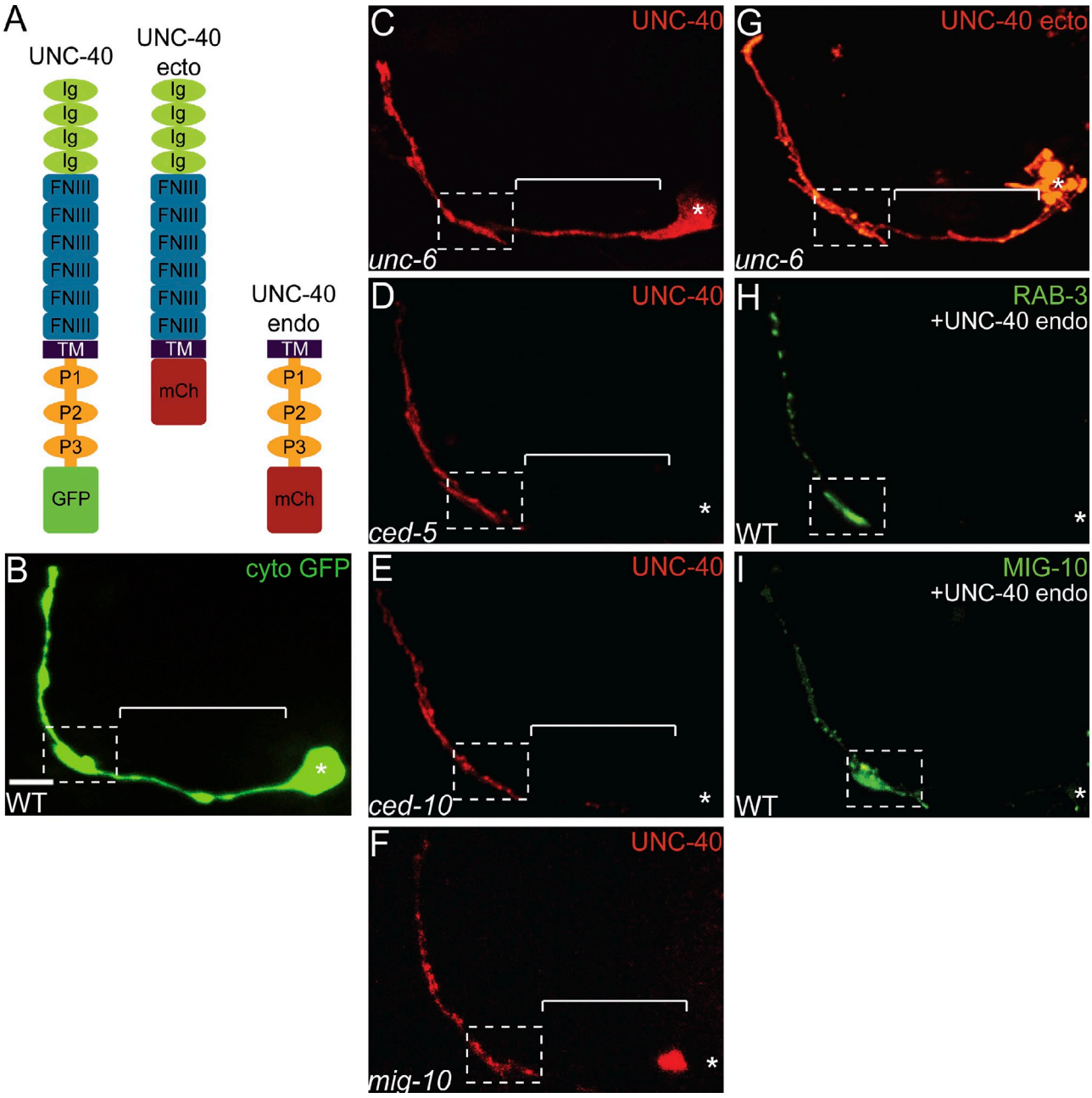

Figure S3. **Localization of UNC-40 to presynaptic regions is dependent on UNC-6.** (A) Diagram of the examined UNC-40 protein constructs. In all cartoons: Ig, Immunoglobulin domain; FNIII, Fibronectin type III repeat; TM, transmembrane domain; GFP, green fluorescent protein; mCh, mCherry. (B) Representative micrograph of a transgenic animal expressing cytoplasmic GFP cell specifically in AIY. (C–F) Representative micrographs of transgenic animals expressing UNC-40::GFP cell specifically in AIY in *unc-6(ev400)* (C), *ced-5(n1812)* (D), *ced-10(n3246)* (E), and *mig-10(ct41)* (F) mutants. Note the UNC-40::GFP is diffusely localized throughout the neurite, including asynaptic Zone 1, in *unc-6(ev400)* mutants (compare with Fig. 1 F), but not in *ced-5, ced-10* and *mig-10* mutants. (G) Cell-specific expression in AIY of UNC-40 ectodomain::mCh in *unc-6(ev400)* mutants. Note the UNC-40 ectodomain::mCh is diffusely localized throughout the neurite, including asynaptic Zone 1, in *unc-6(ev400)* mutants (compare with Fig. 1 G). (H–I) AIY-specific expression of UNC-40 endodomain::mCh in wild-type animals expressing GFP::RAB-3 (H) and MIG-10::GFP (I). Note that localization of the downstream components is not disturbed by overexpression of UNC-40 endo::mCh (compare with Figs. 1 B and 5 A, respectively). In all images, dashed box encloses Zone 2 and bracket indicates the asynaptic Zone 1 region of the AIY neurite. The asterisk represents location of the cell body. Bar, 5 µm.

Published March 26, 2012

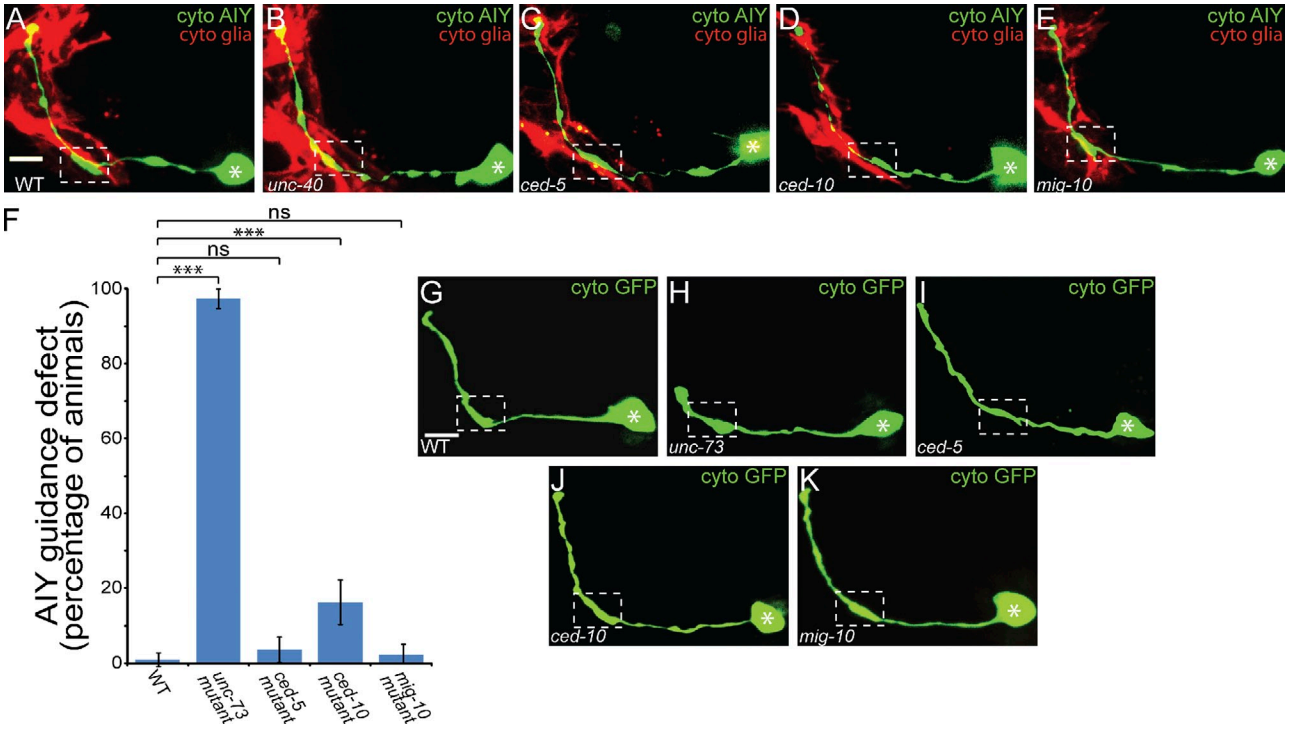

Figure S4. **AIY cell migration and axon guidance in examined mutant backgrounds.** (A–E) Confocal maximal projections of AIY morphology as visualized by the cell-specific expression (*ttx-3* promoter) of cytoplasmic GFP and the glial cell morphology as visualized by the cell-specific expression (*hlh-17* promoter) of cytoplasmic mCherry in wild-type (A), *unc-40(e271)* (B), *ced-5(n1812)* (C), *ced-10(n3246)* (D), and *mig-10(ct41)* (E) mutants. We did not detect abnormalities in the position of the AIY with regards to glia in the examined mutants. Bar (A–E), 5 µm. (F) Quantification of AIY axon guidance defects in wild-type (n = 109), *unc-73(e936)* (n = 148), *ced-5(n1812)* (n = 113), *ced-10(n3246)* (n = 148), and *mig-10(ct41)* (n = 131) mutants. Quantification of the axon guidance or cell migration phenotype in AIY was conducted as described previously (Colón-Ramos et al., 2007). In brief, animals were closely examined and scored for the cell migration of the AIY cell body to the retrovesicular ganglion and the three navigational decisions AIY makes as it traverses the ventral nerve cord and the nerve ring: (1) anterior projection through the ventral nerve cord, (2) dorsal turn at the nerve ring, and (3) circumnavigation of the nerve ring until the AIY neurite contacts the sister AIY at the dorsal midline. In *ced-10* mutants, 16.2% of mutant animals displayed axon truncations in AIY. No other notable guidance or axon truncation defects were observed for *ced-5(n1812)* or *mig-10(ct41)* mutants. ***, $P < 0.0001$ between indicated groups. Error bars represent 95% confidence interval. (G–K) Confocal maximal projections of AIY morphology as visualized by the cell-specific expression of cytoplasmic GFP in wild-type (G), *unc-73(e936)* (H), *ced-5(n1812)* (I), *ced-10(n3246)* (J), and *mig-10(ct41)* (K) mutants. Note that only *unc-73(e936)* mutants exhibit axon truncations (H); other pathway mutant animals (I–K) demonstrate axon guidance similar to wild type (G) in most animals (F). Bar (G–K), (5 µm). In all images, dashed box encloses Zone 2 and asterisk represents location of the cell body.

Published March 26, 2012

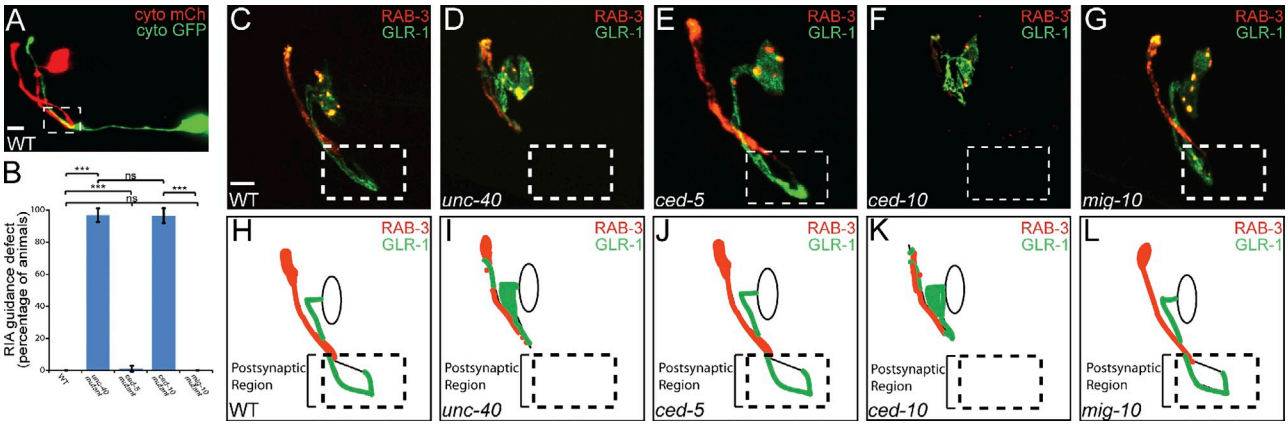

Figure S5. **UNC-40 instructs guidance in postsynaptic neuron RIA through a distinct downstream signaling pathway.** (A) Confocal micrograph of a representative adult with presynaptic AIY (green) and postsynaptic RIA (red). The region where RIA is innervated by AIY is highlighted with a dashed box. Bar, 5 µm. (B) Quantification of abnormal guidance of RIA in wild-type (n = 66), *unc-40(e271)* (n = 64), *ced-5(n1812)* (n = 105), *ced-10(n3246)* (n = 58), and *mig-10(ct41)* (n = 59) mutant animals. (C–L) RIA morphology, presynaptic distribution, and postsynaptic distribution are assayed with a transgenic line that cell-specifically expresses the presynaptic marker mCh::RAB-3 and the postsynaptic glutamate receptor GLR-1::GFP (Margeta et al., 2009). RIA projects ventrally to be innervated by AIY at Zone 2 (dashed box). In *unc-40(e271)* and *ced-10(n3246)* mutant animals, RIA fails to project ventrally to Zone 2 (D, F, I, and K). In *ced-5(n1812)* and *mig-10(ct41)* mutant animals, RIA projects as in wild type and the relative distribution of pre- and postsynaptic specializations are indistinguishable from that seen in wild-type animals (E, G, J, and L). Our observation that CED-5 and MIG-10 are not required for RIA axon guidance suggests that the UNC-40–mediated synaptic vesicle clustering mechanisms in AIY are genetically separable from the UNC-40–mediated axon guidance mechanisms in RIA.***, $P < 0.0001$ between indicated groups. Bar (C–G), 5 µm.

References

Colón-Ramos, D.A., M.A. Margeta, and K. Shen. 2007. Glia promote local synaptogenesis through UNC-6 (netrin) signaling in *C. elegans*. *Science*. 318:103–106. http://dx.doi.org/10.1126/science.1143762

Margeta, M.A., G.J. Wang, and K. Shen. 2009. Clathrin adaptor AP-1 complex excludes multiple postsynaptic receptors from axons in *C. elegans*. *Proc. Natl. Acad. Sci. USA*. 106:1632–1637. http://dx.doi.org/10.1073/pnas.0812078106